

Bypassing mitochondrial defects rescues Huntington's phenotypes in *Drosophila*

Susanna Campesan^{a,*}, Ivana del Popolo^a, Kyriaki Marcou^a, Anna Straatman-Iwanowska^b, Mariaelena Repici^{a,c}, Kalina V. Boytcheva^a, Victoria E. Cotton^a, Natalie Allcock^b, Ezio Rosato^a, Charalambos P. Kyriacou^a, Flaviano Giorgini^{a,*}

^a Department of Genetics and Genome Biology, University of Leicester, Leicester LE1 7RH, UK

^b Electron Microscopy Facility, Core Biotechnology Services, Adrian Building, University of Leicester, University Road, Leicester LE1 7RH, Leicestershire, UK

^c School of Life and Health Sciences, Aston University, Aston Triangle, Birmingham B4 7ET, UK

ARTICLE INFO

Keywords:

Huntington's disease
Mitochondrial dysfunction
Parkin
Huntingtin
Neurodegeneration

ABSTRACT

Huntington's disease (HD) is a fatal neurodegenerative disease with limited treatment options. Human and animal studies have suggested that metabolic and mitochondrial dysfunctions contribute to HD pathogenesis. Here, we use high-resolution respirometry to uncover defective mitochondrial oxidative phosphorylation and electron transfer capacity when a mutant huntingtin fragment is targeted to neurons or muscles in *Drosophila* and find that enhancing mitochondrial function can ameliorate these defects. In particular, we find that co-expression of parkin, an E3 ubiquitin ligase critical for mitochondrial dynamics and homeostasis, produces significant enhancement of mitochondrial respiration when expressed either in neurons or muscles, resulting in significant rescue of neurodegeneration, viability and longevity in HD model flies. Targeting mutant HTT to muscles results in larger mitochondria and higher mitochondrial mass, while co-expression of parkin increases mitochondrial fission and decreases mass. Furthermore, directly addressing HD-mediated defects in the fly's mitochondrial electron transport system, by rerouting electrons to either bypass mitochondrial complex I or complexes III-IV, significantly increases mitochondrial respiration and results in a striking rescue of all phenotypes arising from neuronal mutant huntingtin expression. These observations suggest that bypassing impaired mitochondrial respiratory complexes in HD may have therapeutic potential for the treatment of this devastating disorder.

1. Introduction

Huntington's disease (HD) is a fatal neurodegenerative disorder characterised by involuntary movements, personality changes, and dementia, which affects approximately 11–14 per 100,000 of the population (McColgan and Tabrizi, 2018). HD is caused by a CAG trinucleotide repeat expansion encoding a polyglutamine stretch in the huntingtin (HTT) protein, leading to its aggregation and the dysfunction/death of vulnerable neurons (Ross and Tabrizi, 2011). Metabolic dysfunction is a feature of HD pathology, underlined by patient weight loss (Aziz et al., 2008), decreased glucose metabolism and increased lactate concentrations in the brain (Jenkins et al., 1993; Antonini et al., 1996; Feigin et al., 2001; Reynolds Jr. et al., 2005). Moreover, deficiency of the mitochondrial respiratory chain complex II (succinate dehydrogenase -SDH), has been linked to HD as SDH inhibition by 3-nitropropionate

closely mimics HD neuropathology and clinical features in primates (Palfi et al., 1996) and rodents (Brouillet et al., 1998). HD *post-mortem* studies have revealed abnormal mitochondrial morphology in the cerebral cortical tissue of symptomatic HD patients (Goebel et al., 1978; Tellez-Nagel et al., 1974) and subsequent studies showed that the activity of the electron transport complexes II, III and IV are reduced in the caudate or putamen, the brain regions most affected by HD (Browne et al., 1997). Studies in peripheral human tissues such as blood cells or muscle biopsies have also found structural abnormalities in mitochondria (Squitieri et al., 2006; Squitieri et al., 2010), ATP deficiencies (Lodi et al., 2000) and impairments of the electron transfer chain particularly involving complex I (Ehinger et al., 2016; Mejia et al., 2016).

While HD animal models have produced contrasting results on mitochondrial dysfunction (Polyzos and McMurray, 2017), mitochondrial and energetic defects are major features of disease progression

* Corresponding authors.

E-mail addresses: sc17@le.ac.uk (S. Campesan), fg36@le.ac.uk (F. Giorgini).

<https://doi.org/10.1016/j.nbd.2023.106236>

Received 6 June 2023; Received in revised form 6 July 2023; Accepted 22 July 2023

Available online 24 July 2023

0969-9961/© 2023 The Authors. Published by Elsevier Inc. This is an open access article under the CC BY license (<http://creativecommons.org/licenses/by/4.0/>).

(Browne, 2008). Many cellular functions compromised during HD progression (e.g. vesicular trafficking, autophagy, synaptic signalling, oxidative damage repair) rely on an efficient supply of energy, and could be the result of, or be amplified by, mitochondrial and energetic defects. In addition to alterations in mitochondrial energy metabolism, several reports have found anomalous mitochondrial trafficking and dynamics in various HD models (Yano et al., 2014; Mason et al., 2013; Orr et al., 2008; Trushina et al., 2004; Song et al., 2011; Costa et al., 2010).

Parkin is a cytosolic E3 ubiquitin ligase, mutations of which are known to cause Parkinson's disease (PD) (Shimura et al., 2000). Studies in *Drosophila* and cells have observed that *parkin* mutations cause the accumulation of dysfunctional mitochondria, indicating a role in mitochondrial dynamics and quality control (Greene et al., 2003; Park et al., 2006; Clark et al., 2006; Yang et al., 2006; Deng et al., 2008; Narendra et al., 2008; Gegg et al., 2010; Narendra et al., 2010; Vives-Bauza et al., 2010; Ziviani et al., 2010). Parkin is recruited and activated onto dysfunctional mitochondria by the Ser/Thr kinase PTEN-induced kinase 1 (PINK1), leading to the ubiquitination of several mitochondrial outer membrane proteins, including the mammalian profusion factors mitofusin (Mfn) 1 and 2 and the *Drosophila* single profusion factor *Marf* (Sandoval et al., 2014), which results in promoted fission and autophagic degradation of dysfunctional mitochondria (mitophagy) (Gegg et al., 2010; Ziviani et al., 2010; Tanaka et al., 2010; Glauser et al., 2011; Rakovic et al., 2011; Youle and Narendra, 2011). Ubiquitous and pan-neuronal upregulation of parkin in wild-type *Drosophila* was shown to extend lifespan by reducing proteotoxicity, altering mitochondrial dynamics and enhancing mitochondrial metabolism (Rana et al., 2013).

Here we uncover significant mitochondrial functional defects in neurons and muscles of HD flies and show that these and all other HD-related neuronal dysfunctions can be rescued by parkin upregulation. We also bypass mitochondrial defects in HD flies by utilising the NADH-quinone oxidoreductase Ndi1 from *S. cerevisiae* (Small and McAlister-Henn, 1998; De Vries et al., 1992). This single subunit NADH-quinone oxidoreductase, located on the matrix side of the inner mitochondrial membrane is insensitive to complex I inhibitors, and, when transgenically expressed, is able to compensate for respiratory deficiencies caused by defects in the host complex I (NADH-quinone oxidoreductase). Ndi1 has therefore been shown to restore NADH oxidation in cell lines (Seo et al., 2000), flies (Cho et al., 2012; Vilain et al., 2012) and mice (Seo et al., 2006).

Similarly, we employed an alternative oxidase (AOX) found in the mitochondria of several invertebrates, plants and fungi (McDonald and Vanlerberghe, 2004; McDonald and Vanlerberghe, 2006). AOX is a single subunit ubiquinol oxidase, able to transfer electrons directly from the reduced ubiquinone to oxygen, bypassing both complex III and IV (Juszczuk and Rychter, 2003). AOX from *C. intestinalis* has been shown to complement cytochrome *c* oxidase (complex IV) deficiency in human cells (Hakkaart et al., 2006; Dassa et al., 2009a; Dassa et al., 2009b), to rescue *Drosophila* complex III and IV deficiencies (Fernandez-Ayala et al., 2009) and to bypass cytochrome *c* oxidase blockade and lower mitochondrial reactive oxygen species (mtROS) in mice (El-Khoury et al., 2013). We therefore expressed Ndi1 or AOX in mutant HD flies in order to circumvent defects in complex I or III-IV and observed that in both cases there was a significant increase in mitochondrial respiration and a striking rescue of all the phenotypes associated with expression of mutant huntingtin.

2. Results

2.1. Pan-neuronal expression of parkin in HD flies significantly increases mitochondrial respiration and rescues neurodegeneration, viability and longevity

In *Drosophila*, *elavGAL4*-driven pan-neuronal expression of a mutant human HTT exon 1 fragment coding for 93 glutamines (HTT93Q, *elav* > *HTT93Q*) results in progressive loss of neuronal cells (rhabdomeres) in

the eyes, reduced viability and longevity (Pallos et al., 2008; Steinert et al., 2012). Here we used high resolution respirometry (see Methods) to uncover mitochondrial defects and observed that HTT93Q expression in neurons (*elav* > *HTT93Q*) was associated with significant respiration defects, with mitochondrial leak (LEAK) (Fig. 1A), oxidative phosphorylation (oxphos) capacity linked to complex I (P CI), complex I plus II (P CI + II) and complex I plus II plus glycerol phosphate dehydrogenase (P CI + II + GP) all significantly reduced in 9-day old HTT93Q female flies compared to controls (Fig. 1B). Similarly, the electron transfer capacity through complex I plus II plus glycerol phosphate dehydrogenase (ETS CI + II + GP), that of complex II (ETS CII) and of complex IV (ETS CIV) were all significantly reduced in HTT93Q (Fig. 1B). Mitochondrial loss of cytochrome *c* was also measured as the relative increase in complex IV ETS capacity when excess cytochrome *c* was added to the respiration buffer (Δ CYTC). Although loss of cytochrome *c* can occur during sample preparation, we found that samples from HTT93Q flies consistently had significantly higher Δ CYTC measurements than controls (Fig. 1B).

Co-expression of parkin in HTT93Q neurons (*elav* > *HTT93Q* + *park*) did not significantly change the LEAK (Fig. 1A), but rescued all the defects of the complexes analysed, including the oxphos capacities (P CI, P CI + II, P CI + II + GP) and electron transfer system capacities (ETS CI + II + GP, ETS CII, ETS CIV) (Fig. 1B). Expression of parkin in neurons also lowered the higher Δ CYTC observed in HD flies (Fig. 1B). Similar results were observed when using a homogenate from five flies for each condition, as opposed to individual flies as above (Fig. S1A, B). Furthermore, significant respiration defects were found as early as 1 day old in males expressing mutant HTT93Q in neurons, and again overexpression of parkin resulted in significant rescue of most of the defects (Fig. S1C, D). Perhaps surprisingly, we observed that overexpression of parkin in wild-type flies (*elav* > *park*) did not significantly alter any of the respiration parameters we studied (LEAK, P CI, P CI + II, ETS CI + II, ETS CII, ETS CIV, Δ CYTC) when compared to controls (*elavGAL4/+*) (Fig. S2A, B).

Pan-neuronal expression of parkin was also found to significantly increase the number of rhabdomeres in HTT93Q flies (*elav* > *HTT93Q* + *park*) at 1 and 7 days of age (~ 50% and ~ 40% rescue, respectively, Fig. 2A, B), significantly increase the number of HTT93Q flies surviving through development and emerging from the pupal case (eclosion %, Fig. 2C) and significantly lengthen their median lifespan (Fig. 2D). Expression of a second, independent MYC-tagged, parkin transgenic line (*elav* > *HTT93Q* + *parkMyc*) also significantly rescued rhabdomere degeneration, eclosion defects and HTT93Q longevity (Fig. S3A–C). The protective effects conferred by expression of either *parkin* transgene were not due to titration of GAL4 as no improvement of any HTT93Q phenotypes were seen when flies co-expressed a *UASdsRed* control transgene (*elav* > *HTT93Q* + *dsRed*) (Fig. S4A–C).

2.2. Pan-neuronal expression of parkin has no effect on levels of pyruvate dehydrogenase or PGC1- α

Zhang et al. (Zhang et al., 2011) reported that parkin regulates the Warburg effect in cells and increases mitochondrial respiration versus glycolysis by upregulating the levels of the pyruvate dehydrogenase (PDH) subunit E1 α 1 (PDHA1). PDH has been shown to be impaired in HD human brains (Sorbi et al., 1983; Butterworth et al., 1985) and the PDH indirect activator dichloroacetate provided protective effects in HD mouse models (Andreassen et al., 2001). We measured levels of PDHA1 in fly heads pan-neuronally expressing HTT93Q (*elav* > *HTT93Q*), HTT93Q + parkin (*elav* > *HTT93Q* + *park*) or parkin alone (*elav* > *park*) and controls (*elavGAL4/+*) and found that overexpression of parkin did not significantly upregulate levels of PDHA1, suggesting it is not a factor in the phenotypes we observed (Fig. S5A, B). Similar results were also obtained in flies when these transgenes were expressed in the muscles using *Mef2GAL4* (Fig. S5C, D).

Abundant evidence suggests that mutant HTT interferes with energy metabolism by transcriptional repression of PGC-1 α (peroxisome

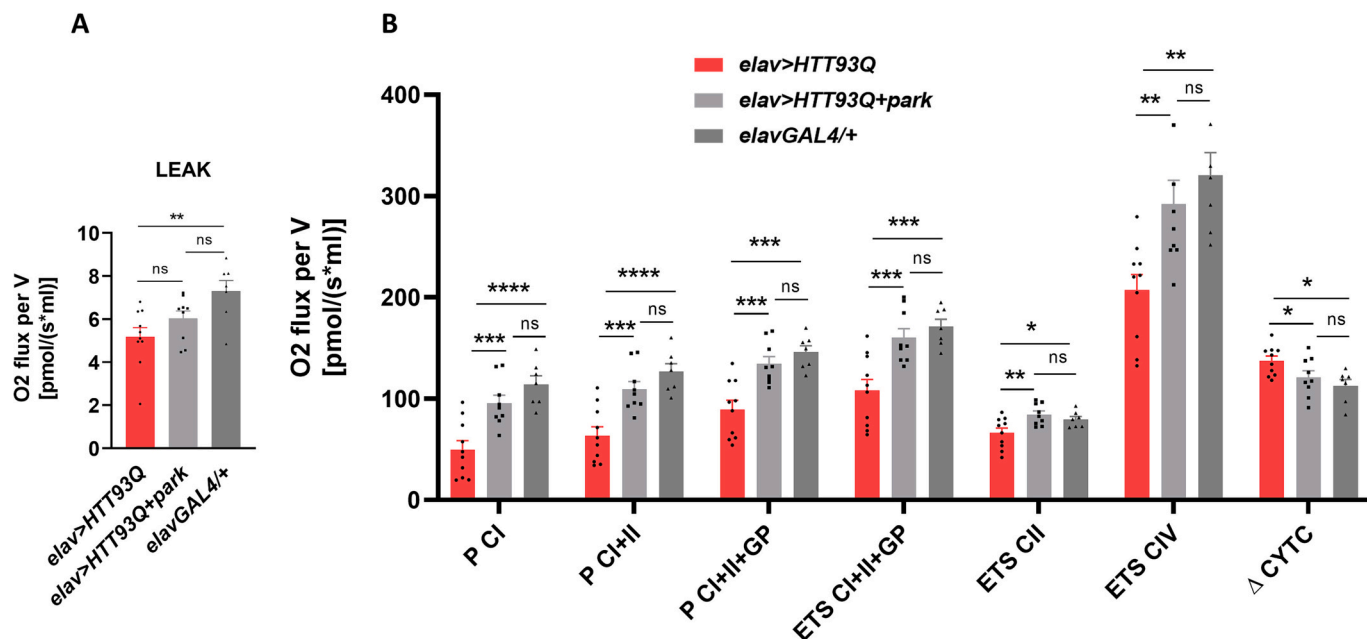


Fig. 1. Overexpression of parkin in HTT93Q neurons rescues mitochondrial respiratory defects. **A:** CI-linked leak is significantly reduced in flies expressing HTT93Q in neurons (*elav > HTT93Q*) compared to controls (*elavGAL4/+*). One-way ANOVA $P = 0.0087$. **B:** Pan-neuronal expression parkin in HTT93Q flies significantly rescues oxphos capacity linked to complex I (PCI), complex I plus complex II (PCI + II) and complex I plus complex II plus glycerol phosphate dehydrogenase (PCI + II + GP) and the electron transfer system capacity linked to complex I plus II plus glycerol phosphate (ETS CI + II + GP), complex II (ETS CII) and complex IV (ETS CIV). The increase in respiration after addition of cytochrome *c* (Δ CYTC), is significantly higher in *elav > HTT93Q* flies and parkin expression significantly lowers this measurement. One-way ANOVA was conducted for each of the seven groups of measurements, all ANOVAs $P < 0.05$ with Newman-Keuls multiple comparison tests. *elav > HTT93Q* ($N = 10$), *elav > HTT93Q + park* (9), *elavGAL4/+* (7), one 9-day old female used per trial.

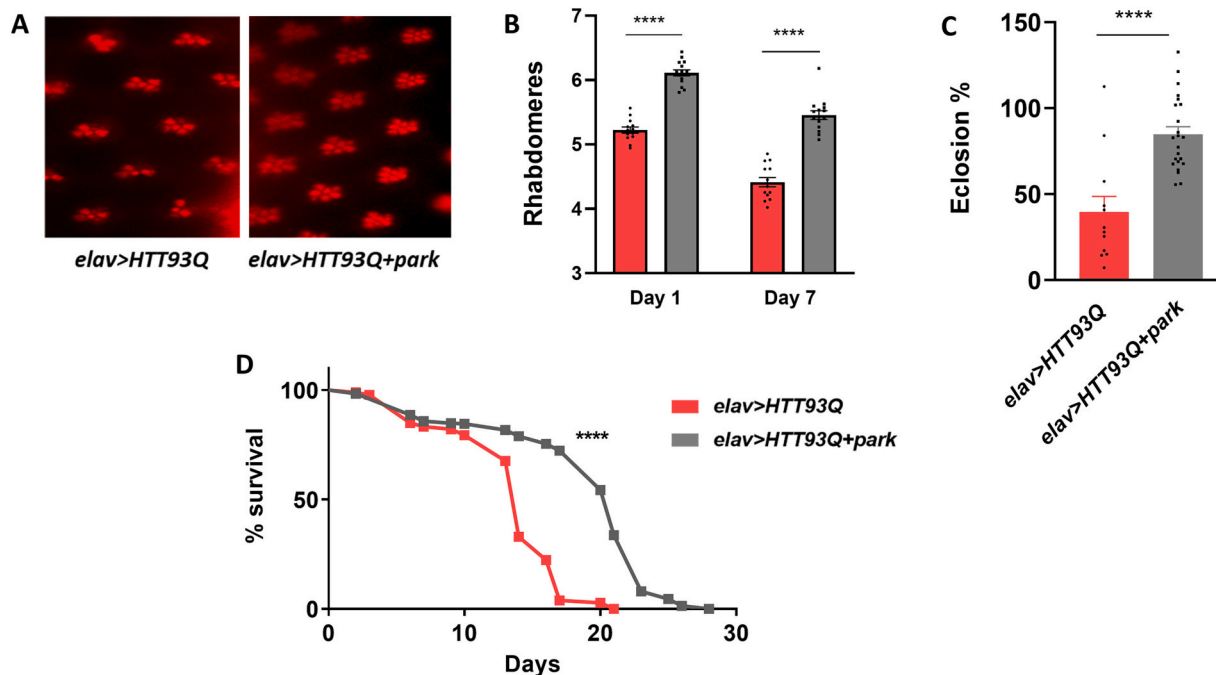


Fig. 2. Neuronal expression of parkin significantly rescues rhabdomere loss, eclosion and longevity defects of HTT93Q flies. **A:** Rhabdomeres. **B:** Average rhabdomeres per ommatidium in HTT93Q (*elav > HTT93Q*) and HTT93Q co-expressing parkin (*elav > HTT93Q + park*). Two-way ANOVA Genotype, Day both $P < 0.0001$. *Post-hoc:* Sidak's multiple comparison test. Day 1 and 14 day 7 *elav > HTT93Q* ($N = 13$), day 1 and day 7 *elav > HTT93Q + park* (15) female flies, at least 50 ommatidia scored per fly. **C:** Eclosion percentages. *t*-test $P < 0.001$. *elav > HTT93Q* (12), *elav > HTT93Q + park* vials (23) in which eclosion was scored. **D:** Comparison of survival curves with log-rank (Mantel-Cox) test $P < 0.001$. *elav > HTT93Q* (179), *HTT93Q + park* (350) virgin females. Panels B, C and D show mean \pm SEM. *post hoc:* *** $P < 0.001$; **** $P < 0.0001$.

proliferator-activated receptor gamma coactivator-1 α), a transcriptional coactivator that regulates several metabolic processes, including mitochondrial biogenesis and oxidative phosphorylation (Puigserver and Spiegelman, 2003; Weydt et al., 2006; Tsunemi and La Spada, 2012). Upregulating PGC-1 α directly or indirectly has been shown to have protective effects in several in vitro and in vivo models of HD (Weydt et al., 2006; Cui et al., 2006; Chiang et al., 2010; Johri et al., 2013). Notably, the levels of PARIS, a repressor of PGC1- α and its target gene NRF-1, are downregulated by the ubiquitin proteasome system after ubiquitination by parkin (Shin et al., 2011; Pirooznia et al., 2020), indicating that parkin function might be involved in maintaining levels of PGC1- α .

We therefore measured levels of the product of *spargel*, the single member of the PGC-1 co-factor family present in *Drosophila*, in fly heads expressing HTT93Q, HTT93Q + parkin, parkin alone or controls. We observed that in this fly model of HD, levels of spargel are not significantly altered compared to wild type, and also that expression of parkin did not significantly increase these levels either in HTT or wild type flies (Fig. S6A, B) indicating that the protection conferred by parkin cannot be attributed to increased levels of PGC1- α .

2.3. Parkin overexpression in HD fly muscles enhances mitochondrial respiration, regulates mitochondrial dynamics and lengthens lifespan

Since HD patients often present bioenergetic deficits and pathology of skeletal muscles (Lodi et al., 2000; Zielonka et al., 2014; Djoussé et al., 2002; Kosinski et al., 2007; Saft et al., 2005), we also measured mitochondrial respiration in two-week old flies expressing HTT93Q in the muscles via the *Mef2GAL4* driver (*Mef2 > HTT93Q*). These flies exhibited highly elevated complex I-linked LEAK. LEAK respiration is measured in the absence of ADP phosphorylation after adding substrates for complex I, and it compensates for proton leak, proton slip and cation cycling, being also influenced by electron leak linked to ROS production (Gnaiger, 2014) (Fig. 3A). *Mef2 > HTT93Q* flies also showed

significantly reduced P CI, P CI + II, P CIV, ETS CI + II, ETS CII and ETS CIV (Fig. 3B) compared to controls (*Mef2GAL4/+*). Furthermore, mitochondrial Δ CYTC was significantly increased in the HTT93Q samples versus controls (Fig. 3B). Overexpression of parkin significantly rescued many of the mitochondrial defects found in HTT93Q muscles. Parkin lowered the high HTT93Q mitochondrial LEAK to control levels (Fig. 3A) and completely rescued P CI, P CI + II and ETS CI + II (Fig. 3B). Parkin overexpression also significantly reduced the Δ CYTC of HD flies to control levels. However, no significant rescue of ETS capacities linked to complex II and complex IV was obtained (Fig. 3B).

Parkin is believed to maintain mitochondrial quality by diverting mitochondrial dynamics towards fission (Gegg et al., 2010; Ziviani et al., 2010; Tanaka et al., 2010; Poole et al., 2010) which encourages the mitophagy of damaged organelles (Deng et al., 2008; Youle and Narendra, 2011). We investigated whether mitochondria in our fly HD model showed any alteration in the balance between fission and fusion and the effects elicited by parkin overexpression. Since fly thoracic flight muscles are rich in mitochondria and generally used to view alterations in mitochondrial dynamics (Deng et al., 2008; Rana et al., 2013; Rana et al., 2017), we compared transmission electron microscopy (TEM) images of these tissues in two-week old flies with *Mef2GAL4*-driven expression of HTT93Q (*Mef2 > HTT93Q*) and HTT93Q + parkin (*Mef2 > HTT93Q + park*) versus controls (*Mef2GAL4/+*) (Fig. 4A). We found that mitochondria in the flight muscles of HTT93Q flies are tightly packed between myofibrils, with few spaces in between (Fig. 4A), and occupy a larger area in each image section analysed when compared to controls (Fig. 4B). Additionally, fewer mitochondria were observed in the sections analysed of HTT93Q (Fig. 4C), indicating a propensity towards mitochondrial fusion. Overexpression of parkin significantly reduced the area occupied by mitochondria in each section analysed to control levels (Fig. 4B), and significantly increased the number of mitochondria (Fig. 4C), suggesting that parkin expression in HD fly muscles was promoting mitochondrial fission.

We also measured the activity of the enzyme citrate synthase (CS) in

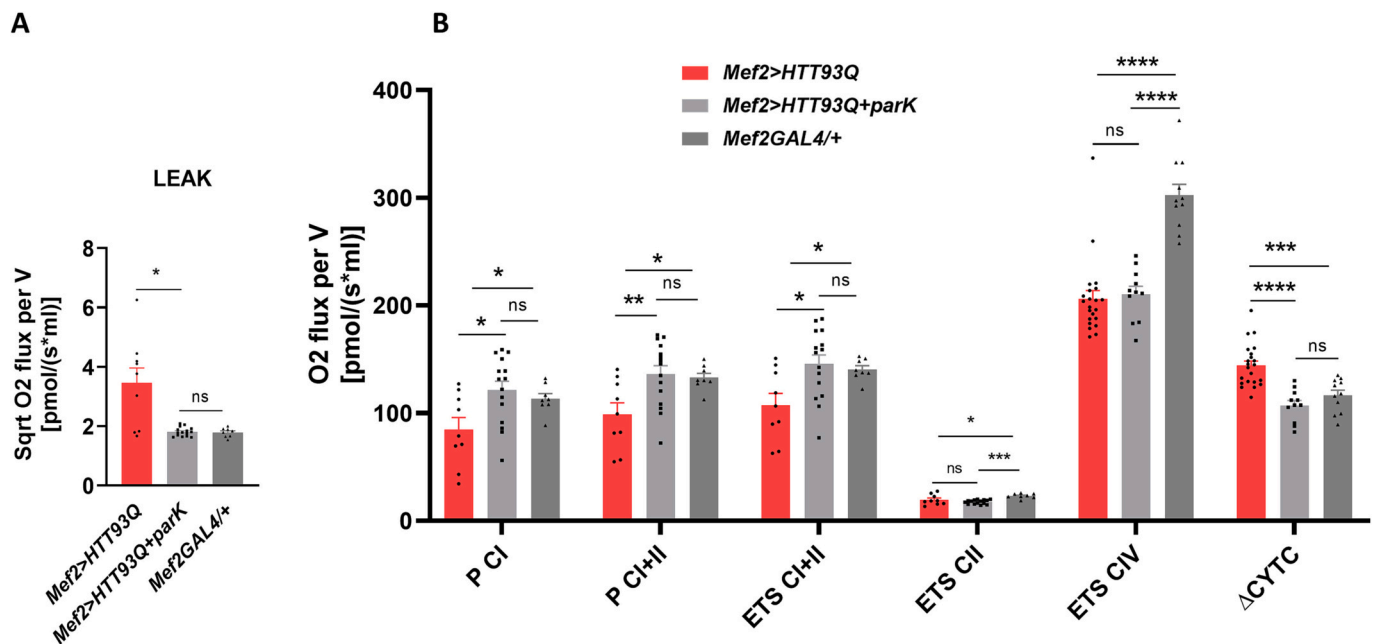


Fig. 3. Overexpression of parkin in HTT93Q muscles rescues several mitochondrial respiratory defects. Parkin overexpression in HTT93Q muscles (*Mef2 > HTT93Q + park*) lowers HTT93Q (*Mef2 > HTT93Q*) mitochondrial leak to control (*Mef2GAL4/+*) levels. Kruskal-Wallis ANOVA $p = 0.023$ with Dunn's multiple comparison test. D: parkin overexpression in HTT93Q muscles completely rescues the oxidative phosphorylation (oxphos) defects linked to complex I (P CI) and complex I plus II (P CI + II) and the electron transfer system capacity of complex I plus II (ETS CI + II). It does not confer any rescue of the complex II (ETS CII) and IV (ETS CIV), however it lowers Δ CYTC to control levels. One-way ANOVA was conducted for each of the six groups of measurements, all ANOVAs $P < 0.05$ with Newman-Keuls multiple comparison tests. *Mef2 > HTT93Q* ($N = 9$) *Mef2 > HTT93Q + park* (15), *Mef2GAL4/+* (8), one two-week old female used per trial. All panels show mean \pm SEM. ns = not significant; * $P < 0.05$; ** $P < 0.01$; *** $P < 0.001$; **** $P < 0.0001$.

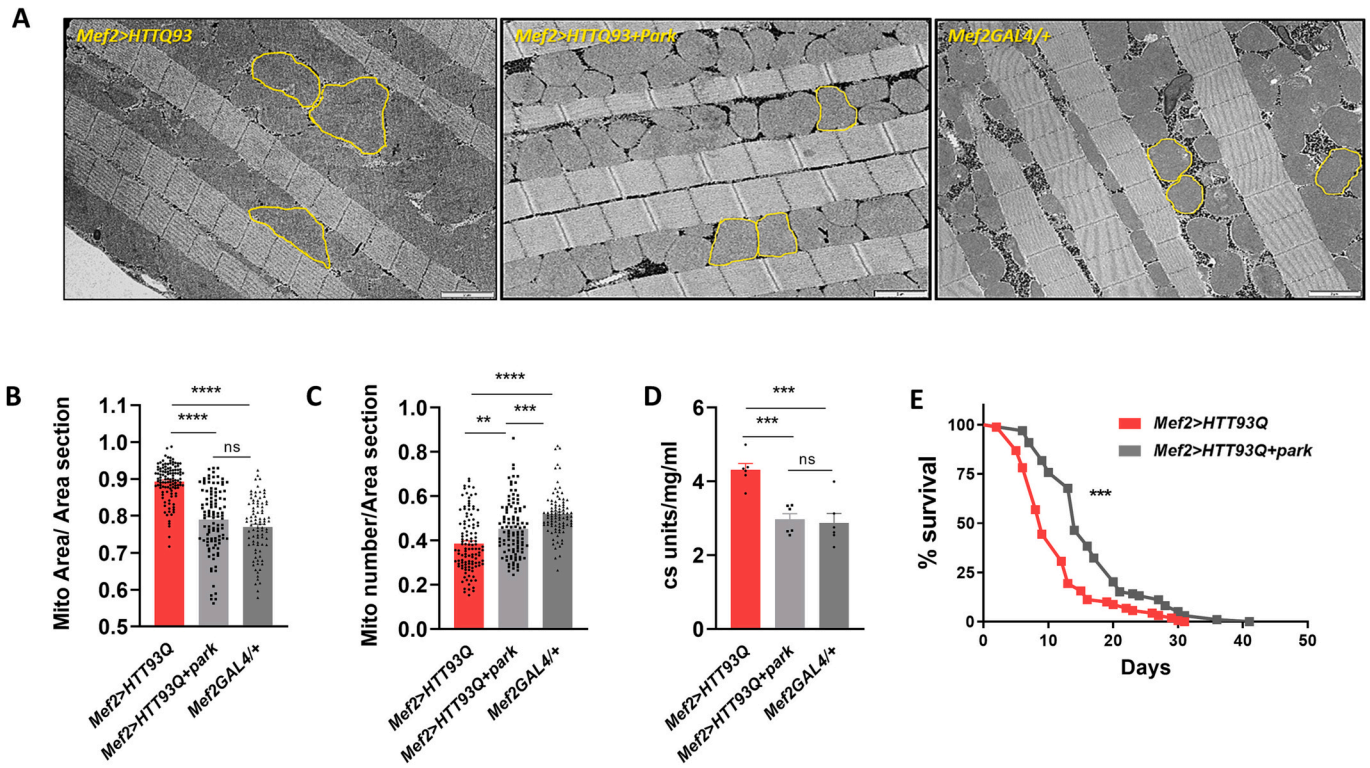


Fig. 4. Parkin overexpression in muscles alters mitochondrial dynamics and significantly increases HTT93Q flies longevity. **A:** Transmission electron microscope images of mitochondria within muscles fibers of HTT93Q (*Mef2 > HTT93Q*), HTT93Q co-expressing parkin (*Mef2 > HTT93Q + park*) and control (*Mef2GAL4/+*) two-week old female flies. The yellow contours highlight some of the mitochondria in each image. Scale bar = 2 μ m. **B:** The area occupied by mitochondria over the area of each analysed section is significantly higher in HTT93Q flies compared to controls. Overexpression of parkin reduces this value to control levels. One-way ANOVA $P < 0.0001$ with Tukey's multiple comparison test. **C:** The number of mitochondria per section analysed is significantly lower in HTT93Q than in controls and expression of parkin significantly increases this value. One-way ANOVA $P < 0.0001$ with Tukey's multiple comparison test. $N = 3$ fly thoraces per genotype. *Mef2 > HTT93Q* = fly 1: 390 mitochondria and 32 sections, fly 2: 288 mitochondria and 34 sections, fly 3: 336 mitochondria and 49 sections analysed. *Mef2 > HTT93Q + park* = fly 1: 405 mitochondria and 29 sections, fly 2: 390 mitochondria and 34 sections, fly 3: 743 mitochondria and 43 sections analysed. *Mef2GAL4/+* = fly 1: 285 mitochondria and 25 sections, fly 2: 203 mitochondria and 27 sections, fly 3: 491 mitochondria and 37 sections analysed. **D:** The activity of the enzyme citrate synthase is significantly higher in HTT93Q fly samples than in controls and expression of parkin lowers this value to control levels. One-way ANOVA $P = 0.0002$ with Tukey's multiple comparison test. $N = 6$ biological and 3 technical repeats per genotype. **E:** Overexpression of parkin in HTT93Q muscles significantly increases longevity. Comparison of survival curves with log-rank (Mantel-Cox) test $P < 0.001$. *Mef2 > HTT93Q* ($N = 160$), *Mef2 > HTT93Q + park* (100) virgin females. Panels B, C and D show mean \pm SEM. ns = not significant, *** $P < 0.001$; **** $P < 0.0001$. (For interpretation of the references to colour in this figure legend, the reader is referred to the web version of this article.)

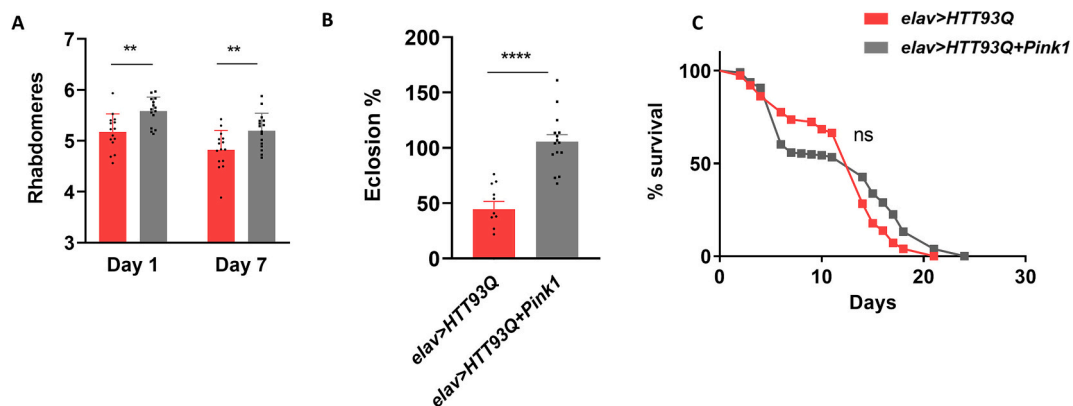


Fig. 5. Pan-neuronal expression of Pink1 in HTT93Q flies rescues rhabdomere loss and eclosion defects but does not significantly increase lifespan. **A:** Pan-neuronal expression of Pink1 (*elav > HTT93Q + Pink1*) significantly rescues HTT93Q (*elav > HTT93Q*) rhabdomere loss. Two-way ANOVA Genotype $P < 0.0001$, Day $P = 0.0001$. Sidak's multiple comparison test. $N = 15$ day 1 and day 7 female flies per genotype, at least 50 ommatidia scored per fly. **B:** Neuronal expression of Pink1 significantly rescues HTT93Q eclosion percentages. t-test $P < 0.0001$. *elav > HTT93Q* ($N = 11$ tubes scored), *elav > HTT93Q + Pink1* (15). **C:** Overexpression of Pink1 does not increase HTT93Q flies longevity. Comparison of survival curves with log-rank (Mantel-Cox) test not significant. *elav > HTT93Q* (150), *elav > HTT93Q + Pink1* (200) virgin females. Panels A and B show mean \pm SEM. ns = not significant; * $P < 0.05$; ** $P < 0.01$; **** $P < 0.0001$.

two-week old flies of the above genotypes. CS activity is directly proportional to, and is often used as a measure of mitochondrial mass (Gegg et al., 2010; Larsen et al., 2012; Watts et al., 2004; Hargreaves et al., 2007). In line with our observations from the TEM images, we found that the CS activity of HTT93Q flies was significantly greater than that of controls and overexpression of parkin significantly lowered CS activity to control levels (Fig. 4D). Additionally, parkin upregulation in muscles also resulted in a significant enhancement of lifespan in HD flies (Fig. 4E).

2.4. Pink1 overexpression and genetic alterations of mitochondrial dynamics in HTT93Q flies confer modest protection

Pink1 acts upstream of parkin and is believed to recruit and activate parkin upon mitochondrial dysfunction (Park et al., 2006; Clark et al., 2006; Yang et al., 2006; Deng et al., 2008; Narendra et al., 2008; Gegg et al., 2010; Narendra et al., 2010; Vives-Bauza et al., 2010; Ziviani et al., 2010). Pink1 expression has been shown to ameliorate several HD-related phenotypes both in flies and in mammalian cells (Khalil et al., 2015). We re-explored Pink1 effects on HD flies and observed that pan-neuronal expression of Pink1 (*elav > HTT93Q + Pink1*) significantly rescued HTT93Q associated rhabdomere loss (a rescue of about 20% at day 1 and 7, Fig. 5A) and eclosion defects (Fig. 5B). However, in contrast to a previous report (Khalil et al., 2015), Pink1 expression in neurons failed to increase the longevity of HTT93Q flies (Fig. 5C). Expression of a second Pink1 transgenic line (*elav > HTT93Q(2) + Pink1(3)*) confirmed our initial results (Fig. S7A, B).

As parkin appears to promote fission in HTT93Q flies, we tested if directly enhancing fission could confer neuroprotection. We therefore studied the effects of pan-neuronal expression of the fission promoting protein Drp1 and RNAi downregulation of the *Drosophila* fusion promoting mitofusin, Marf. We found that Drp1 overexpression (*elav > HTT93Q(2) + Drp1*) conferred a slight rescue of rhabdomere loss at day 1 only (~30% rescue) (Fig. 6A), while providing no enhancement of

longevity (Fig. 6B). *Marf* knockdown (*elav > HTT93Q + Marf RNAi*), on the other hand, resulted in significant rescue of rhabdomere loss at both days 1 and 7 (~25% and 30% rescue respectively) (Fig. 6C). However, it provided no rescue of the eclosion defect (Fig. 6D) or HTT93Q longevity (Fig. 6E). These results suggest that increased mitochondrial fission driven pan-neuronally can confer some moderate neuroprotection, but ultimately, this is not sufficient to extend viability nor lifespan of HTT93Q flies to the same extent as HTT93Q flies co-expressing parkin.

In contrast to the results we obtained with parkin, overexpression of neither Pink1 (*Mef2 > HTT93Q(2) + Pink1(3)*) nor of Drp1 (*Mef2 > HTT93Q(2) + Drp1*) conferred any rescue of the mitochondrial respiration defects found in HTT93Q when expressed in muscles (Fig. S8A, B). When driven in HTT93Q muscles, *Marf2* knockdown resulted in a very severe phenotype with flies dying one or two days post-eclosion so we were unable to proceed further.

2.5. Expression of either an alternative NADH dehydrogenase or an alternative oxidase robustly ameliorates all neuronal HTT93Q defects and significantly increases mitochondrial respiration

As parkin effects in HD flies are associated with the rescue of defective ophos and electron transport capacity, we next investigated the consequence of directly bypassing functional defects of complex I by expressing *Ndi1*. As mentioned above, *Ndi1* is a single unit NADH-quinone oxidoreductase from *S. cerevisiae* which oxidases NADH and reduces ubiquinone, compensating for defects in the function of complex I (also a NADH-quinone oxidoreductase). When co-expressed pan-neuronally with HTT93Q, *Ndi1* (*elav > HTT93Q + Ndi1*) significantly rescued rhabdomere loss (~40% at day 1 and ~30% at day 7) (Fig. 7A), completely reversed the eclosion deficits (Fig. 7B) and very significantly increased the longevity of flies (Fig. 7C).

Similarly, we studied the effects of bypassing complex III and IV via the expression of the alternative oxidase (AOX) from *C. intestinalis*. AOX accepts electrons from the reduced ubiquinone and passes them directly

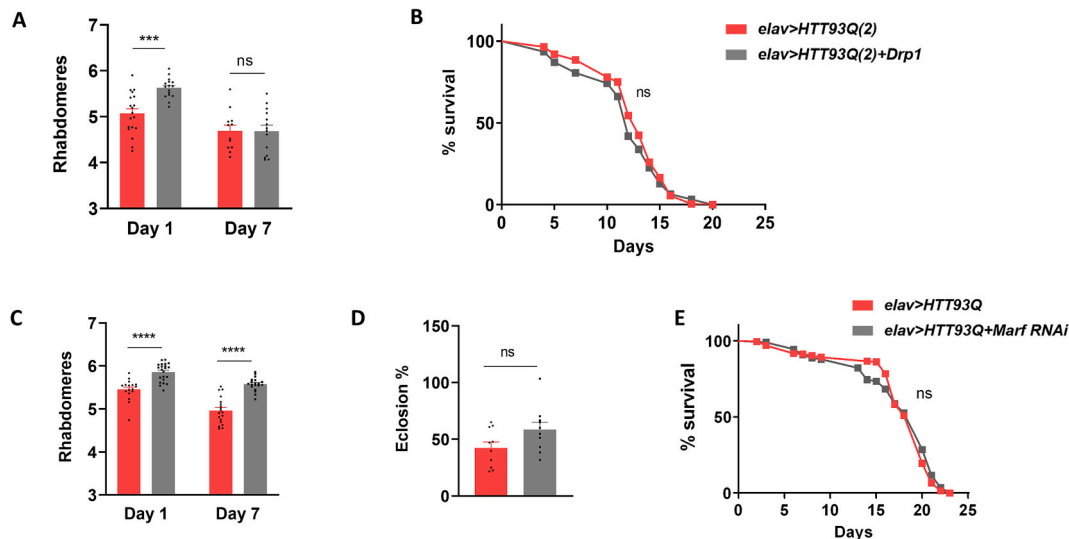


Fig. 6. Pan-neuronal overexpression of Drp1 and downregulation of Marf provide limited rescue of HTT93Q associated phenotypes. A: Overexpression of Drp1 in flies carrying the *HTT93Q* transgene on the second chromosome (*elav > HTT93Q(2) + Drp1*) only significantly increases average rhabdomere numbers per ommatidium in 1 day old flies. Two-way ANOVA Genotype $P = 0.01$, Day $P < 0.0001$, Sidak's multiple comparison. Day 1 ($N = 19$) and day 7 *elav > HTT93Q(2)* ($N = 12$), day 1 (16) and day 7 (14) *elav > HTT93Q(2) + Drp1* female flies, at least 50 ommatidia scored per fly. B: Pan-neuronal expression of Drp1 does not increase longevity of HTT93Q flies. Comparison of survival curves with log-rank (Mantel-Cox) test not significant. *elav > HTT93Q(2)* ($N = 200$), *elav > HTT93Q(2) + Drp1* (60) virgin females. C: Downregulation of Marf in HTT93Q neurons (*elav > HTT93Q + Marf RNAi*) results in a significant rescue of rhabdomere loss both at day 1 and 7 of age. Two-way ANOVA Genotype, Day, both $P < 0.0001$, Sidak's multiple comparison. Day 1 (17) and day 7 (19) *elav > HTT93Q*, day 1 (22) and day 7 (19) *elav > HTT93Q + Marf RNAi* female flies, at least 50 ommatidia scored per fly. D: Downregulation of Marf does not rescue HTT93Q eclosion deficit. t-test not significant. $N = 20$ tubes scored per genotype. E: Pan-neuronal downregulation of Marf in HTT93Q does not increase longevity. Comparison of survival curves with log-rank (Mantel-Cox) test not significant. *elav > HTT93Q* ($N = 190$), *elav > HTT93Q + Marf* (200) *RNAi* virgin females. Panels A, C and D show mean \pm SEM. ns = not significant; *** $P < 0.001$; **** $P < 0.0001$.

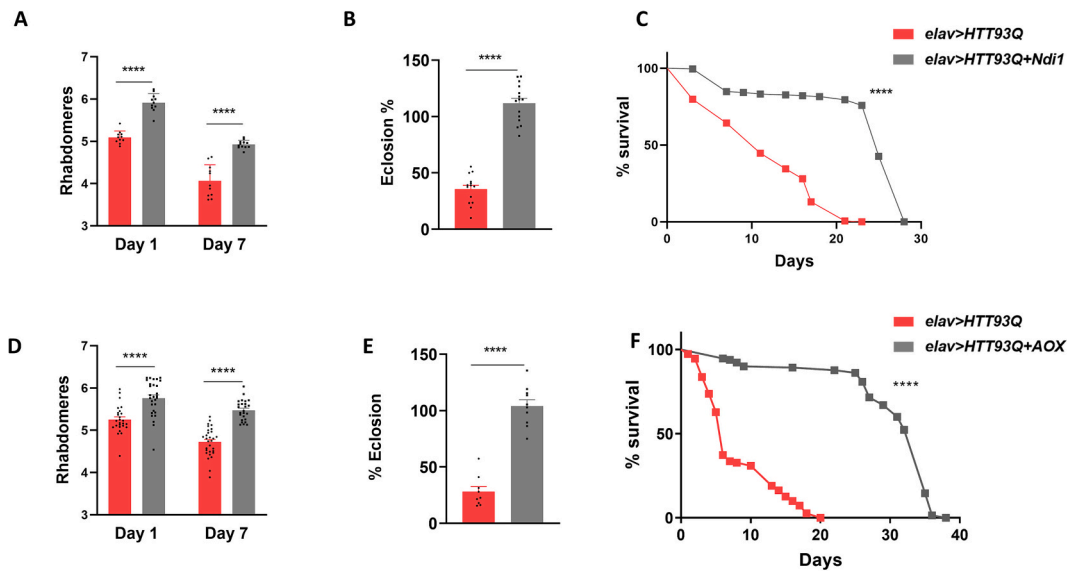


Fig. 7. Pan-neuronal expression of Ndi1 or AOX significantly rescues HTT93Q associated rhabdomere loss, eclosion and longevity defects. **A:** Average rhabdomeres per ommatidium in HTT93Q (*elav > HTT93Q*) and HTT93Q co-expressing Ndi1 (*elav > HTT93Q + Ndi1*). Two-way ANOVA Genotype, Day both $P < 0.0001$, Sidak's multiple comparison. day1 ($N = 11$) and day7 *elav > HTT93Q*, day1 (11) and day7 (12) *elav > HTT93Q + Ndi1* female flies, at least 50 ommatidia scored per fly. **B:** Eclosion percentages. t-test $P < 0.0001$. $N = 14-15$ vials scored per genotype. **C:** Comparison of survival curves with log-rank (Mantel-Cox) test $P < 0.0001$. *elav > HTT93Q* ($N = 168$), *elav > HTT93Q + Ndi1* (190) virgin females. **D:** Average rhabdomeres per ommatidium in 1 day and 7 days old HTT93Q (*elav > HTT93Q*) and HTT93Q co-expressing AOX (*elav > HTT93Q + AOX*). Two-way ANOVA Genotype, Day both $P < 0.0001$, Sidak's multiple comparison. day1 (26) and day 7 (30) *elav > HTT93Q*, day 1 (29) and day 7 (25) *elav > HTT93Q + AOX* female flies, at least 50 ommatidia scored per fly. **E:** Eclosion percentages of HTT93Q (*elav > HTT93Q*) and HTT93Q co-expressing AOX (*elav > HTT93Q + AOX*). t-test $P < 0.0001$. *elav > HTT93Q* ($N = 9$) and *elav > HTT93Q + AOX* (10) vials scored. **F:** Comparison of survival curves with log-rank (Mantel-Cox) test $P < 0.0001$. *elav > HTT93Q* (110), *elav > HTT93Q + AOX* (130) virgin females. Panels A, B, D and E show mean \pm SEM. **** $P < 0.0001$.

to oxygen, therefore rerouting electrons away from complex III and IV. The ubiquinone pool is a major site of reactive oxidant species (ROS) production along the respiratory chain, and the formation of superoxide is significantly increased by compounds, such as antimycin A, which block the electron transport downstream of ubiquinone. Rerouting electrons from defective complexes III/IV, via AOX, would then prevent over-reduction of the ubiquinone pool, decreasing the risk of electrons escaping to form superoxide (Maxwell et al., 1999). We observed that pan-neuronal expression of AOX in HTT93Q flies (*elav > HTT93Q + AOX*) significantly rescued HTT93Q rhabdomere loss (~30% rescue at

day 1 and 7) (Fig. 7D), completely rescued eclosion defects (Fig. 7E) and very significantly increased the survival of HTT93Q flies (Fig. 7F). The expression of a second transgenic AOX line (*elav > HTT93Q + AOXF24*) confirmed these results by also showing significant rescue of all the phenotypes tested (Fig. S9 A-C).

Due to the notable protection conferred by AOX or Ndi1 expression, we next assessed their effects on mitochondrial function via respirometry when targeted to the neurons of HTT93Q flies. We observed that in 3-5 day old females HTT93Q (*elav > HTT93Q*) the CI LEAK was significantly higher than in control *elavGAL4/+* flies (Fig. 8A), while in HD

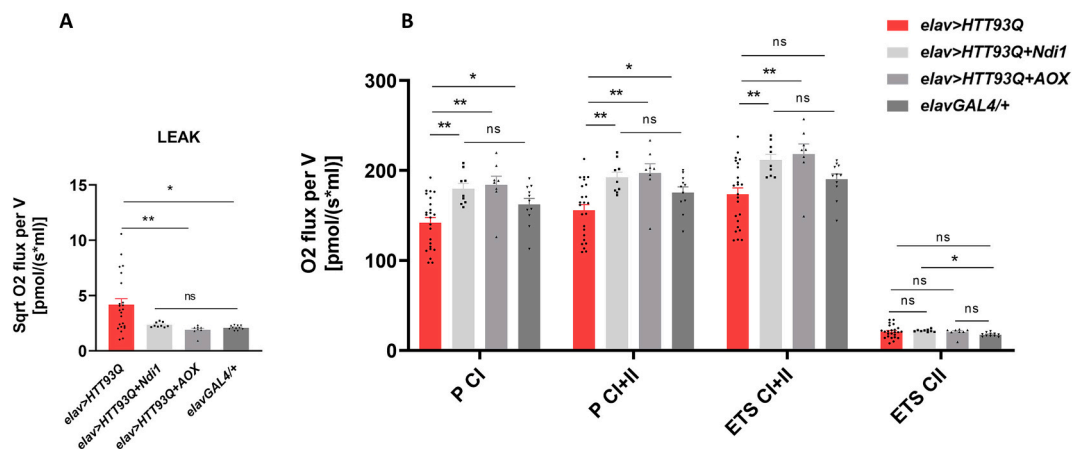


Fig. 8. Pan-neuronal expression of Ndi1 or AOX significantly increase mitochondrial respiration in HD flies. **A:** Leak is significantly higher in HTT93Q (*elav > HTT93Q*) than controls (*elavGAL4/+*). Expression of AOX (*elav > HTT93Q + AOX*) significantly lowers this value. Kruskal-Wallis ANOVA $P = 0.0017$, Dunn's multiple comparison test. **B:** Ndi1 (*elav > HTT93Q + Ndi1*) or AOX (*elav > HTT93Q + AOX*) expression significantly increases HTT93Q complex I and complex I + II-linked OXPHOS (PCI and PCI + II) and ETS through complex I + II (ETS CI + II). ETS through complex II (ETS CII) is significantly increased in samples expressing Ndi1 compared to controls. One-way ANOVA was conducted for each of the four groups of measurements, all ANOVAs $P < 0.05$, Newman-Keuls multiple comparison tests. *elav > HTT93Q* $N = (24)$, *elav > HTT93Q + Ndi1* (9), 8 *elav > HTT93Q + AOX* (8), *elavGAL4/+* (11), one 3-5 day old female fly used per trial. Panels A and B show mean \pm SEM. ns = not significant; * $P < 0.05$; ** $P < 0.01$.

flies co-expressing Ndi1 (*elav > HTT93Q + Ndi1*) or AOX (*elav > HTT93Q + AOX*) the LEAK was comparable to the control (Fig. 8A). Furthermore, the expression of either Ndi1 or AOX resulted in a significant enhancement and complete rescue of the HTT93Q OXPHOS defects measured through complex I (P CI) and complex I + II (P CI + II) (Fig. 8B) and of the electron transfer capacity through complex I and II (ETS CI + II). After inactivation of complex I with rotenone, complex II ETS was also significantly higher in HD flies expressing Ndi1 when compared to controls, likely due to the fact that Ndi1 is resistant to the effects of rotenone (Fig. 8B). Expression of either Ndi1 (*elav > Ndi1*) or AOX (*elav > AOX*) in the neurons of wild type flies also resulted in significantly increased OXPHOS (PCI, P CI + II) and ETS (ETS CI + II, ETS CII) capacities (Fig. S10A, B).

As mentioned above, AOX expression, by diverting electrons from complex III and IV, can prevent over-reduction of the quinone pool and has been associated with lowering of mitochondrial ROS (mtROS) (Juszczuk and Rychter, 2003; Hakkaart et al., 2006; Dassa et al., 2009b; Fernandez-Ayala et al., 2009; El-Khoury et al., 2013). We tested this scenario by using the fluorescent Mitosox probe to measure levels of mtROS in fly brains. We found that, although HTT93Q (*elav > HTT93Q*) expression did not significantly enhance mtROS levels compared to controls (*elavGAL4/+*), expression of AOX in HTT93Q neurons (*elav > HTT93Q + AOX*) was indeed associated with a significant reduction of mtROS when compared to HTT93Q or controls (Fig. 9A, B). In line with these results, reducing mtROS by overexpressing the *Drosophila* superoxide dismutase *Sod2* was also protective, significantly increasing rhabdome number in 7 day old flies (Fig. 9C), rescuing the eclosion

phenotype (Fig. 9D) and significantly increasing longevity in our fly HD model (Fig. 9E). We also noted that parkin overexpression did not significantly reduce the amount of mtROS in HTT93Q flies despite the rescue of neurodegeneration and mitochondrial dysfunction (Fig. 9A, B).

2.6. Combining pan-neuronal expression of parkin and AOX does not result in enhanced rescue of HD phenotypes

We then assessed whether combining pan-neuronal expression of parkin with that of AOX (*elav > HTT93Q + park + AOX*) could further enhance the rescue obtained in HTT93Q flies compared to when each protein was expressed on its own (*elav > HTT93Q + park* or *elav > HTT93Q + AOX*). We found that *elav > HTT93Q + park + AOX* flies did not have a significantly increased number of rhabdomeres either at day 1 or at day 7, when compared to *elav > HTT93Q + park* or *elav > HTT93Q + AOX* flies. In fact, at day 7 the number of rhabdomeres in *elav > HTT93Q + park + AOX* flies was significantly lower than that of *elav > HTT93Q + AOX* flies (Fig. 10A).

The eclosion of *elav > HTT93Q + park + AOX* flies was significantly higher than that of *elav > HTT93Q + park*, but not when compared to that of *elav > HTT93Q + AOX* (Fig. 10B). Expression of AOX and parkin (*elav > HTT93Q + park + AOX*) resulted in very significant enhancement of HD fly lifespan, and it was also significantly more protective than the expression of parkin alone (*elav > HTT93Q + park*) (Fig. 10C). However, surprisingly, the combined expression of parkin and AOX (*elav > HTT93Q + park + AOX*) did not result in further increase of HD fly lifespan when compared to expression of AOX on its own (*elav >*

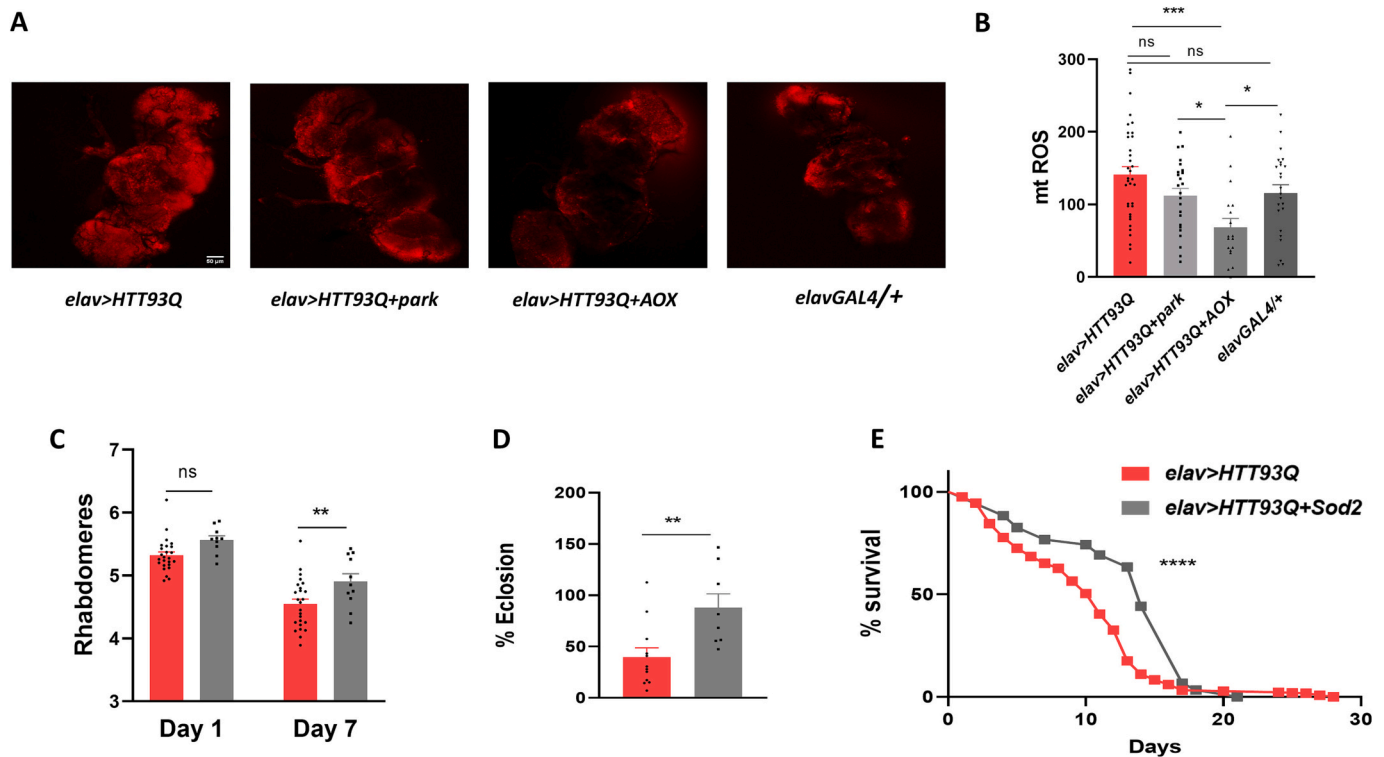


Fig. 9. AOX expression significantly reduces ROS in brains and overexpression of *Sod2* significantly improves HTT93Q phenotypes. **A, B:** Pan-neuronal expression of AOX significantly reduces mitochondrial ROS (mtROS) in fly HTT93Q brains. **A:** Confocal images of female *Drosophila* brains stained with Mitosox. Scale bar = 50 μ m. **B:** Fiji measurements of Mitosox red intensity. One-way ANOVA $P = 0.0004$; Kruskal-Wallis ANOVA $P = 0.0015$, Dunn's multiple comparison test. *elav > HTT93Q* ($N = 35$); *elav > HTT93Q + park* (24); *elav > HTT93Q + AOX* (18); *elavGAL4/+* (24) brains. **C-E:** Pan-neuronal expression of *Sod2* confers protection against HTT93Q associated rhabdomeres loss, eclosion and longevity defects. **C:** Average rhabdomeres per ommatidium in HTT93Q (*elav > HTT93Q*) and HTT93Q co-expressing *Sod2* (*elav > HTT93Q + Sod2*). Two-way ANOVA Genotype $P = 0.0009$, Day $P < 0.0001$, Sidak's multiple comparison test day 1 and day 7 (both $N = 25$) *elav > HTT93Q*, day 1 (10) and day 7 (11) *elav > HTT93Q + Sod2* female flies, at least 50 ommatidia scored per fly. **D:** Eclosion percentages. t-test $P < 0.0001$; *elav > HTT93Q* (12, *elav > HTT93Q + Sod2* (8) vials scored. **E:** Comparison of survival curves with log-rank (Mantel-Cox) test $P < 0.0001$. *elav > HTT93Q* (399), *elav > HTT93Q + Sod2* (120) virgin females. Panels B, C and D show mean \pm SEM. ns = not significant; * $P < 0.05$; ** $P < 0.01$; *** $P < 0.001$; **** $P < 0.0001$. (For interpretation of the references to colour in this figure legend, the reader is referred to the web version of this article.)

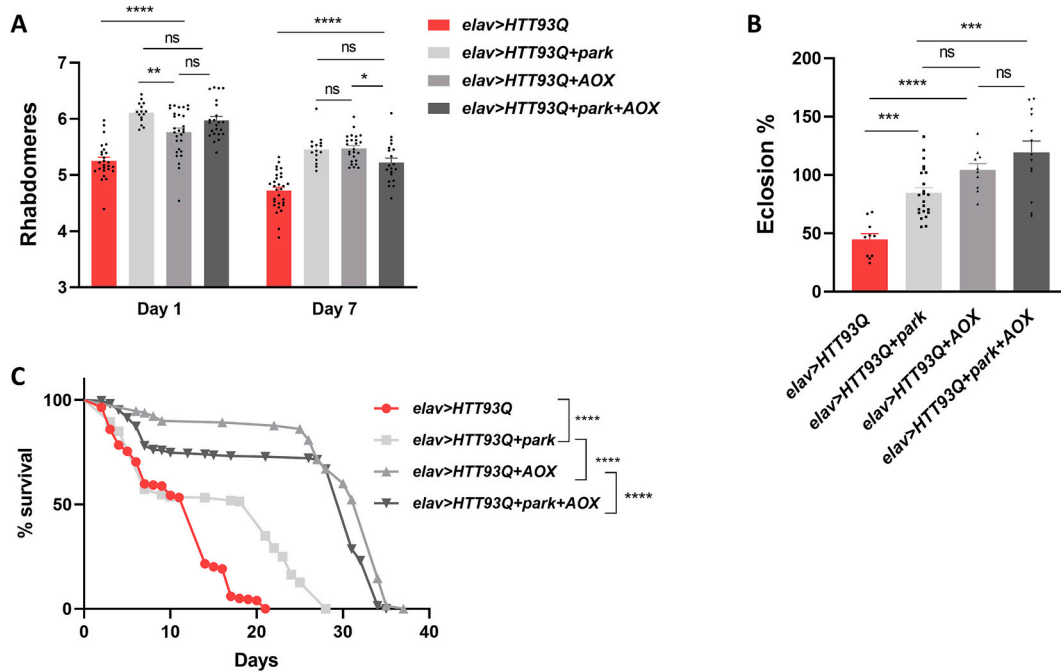


Fig. 10. Combining pan-neuronal expression of parkin and AOX does not result in enhanced rescue of HD phenotypes. A: Average number of rhabdomeres per ommatidium in 1-day and 7-days old HTT93Q (*elav > HTT93Q*), HTT93Q coexpressing parkin (*elav > HTT93Q + park*), HTT93Q coexpressing AOX (*elav > HTT93Q + AOX*) and HTT93Q coexpressing parkin plus AOX (*elav > HTT93Q + park + AOX*). Two-way ANOVA Genotype, Day both $P < 0.0001$. $N = 26$ day 1 and 30 day 7 *elav > HTT93Q*, 15 day 1 and 15 day 7 *elav > HTT93Q + park*, 29 day 1 and 25 day 7 *elav > HTT93Q + AOX*, 23 day 1 and 20 day 7 *elav > HTT93Q + park + AOX* female flies, at least 50 ommatidia scored per fly. B: Eclosion percentages. Anova $P < 0.0001$. $N = 10$ *elav > HTT93Q*, 23 *elav > HTT93Q + park*, 10 *elav > HTT93Q + AOX*, and 13 *elav > HTT93Q + park + AOX* vials scored. C: Comparison of survival curves with log-rank (Mantel-Cox) test $P < 0.0001$. $N = 199$ *elav > HTT93Q*, 220 *elav > HTT93Q + park*, 130 *elav > HTT93Q + AOX*, and 269 *elav > HTT93Q + park + AOX* virgin females. Panels A and B show mean \pm SEM. ns = not significant; * $P < 0.05$; ** $P < 0.01$; *** $P < 0.001$; **** $P < 0.0001$.

HTT93Q + AOX), and actually resulted in a significant reduction of the median lifespan, (although the total lifespan of these two genotypes was similar) (Fig. 10C).

3. Discussion

In this work we find that enhancing mitochondrial function by either overexpressing parkin or bypassing defective mitochondrial complexes has significant beneficial effects in a fly model of HD, rescuing neurodegeneration and enhancing viability and lifespan. Fly models of HD have been extensively characterised and have served as robust models for the study of mutant HTT-dependent neurodegeneration and related phenotypes. In the context of our work herein, the use of fruit flies has provided a useful paradigm for the study of mitochondrial function and its effects on overall health and neurodegeneration *in vivo*, which can now be further considered in mammalian systems. Notably, with the use of high resolution respirometry we uncovered significant defects in the activity of several mitochondrial complexes in HTT flies. Strikingly, parkin upregulation rescues most of these defects when expressed either in neurons or in muscles, albeit with some differences between the two tissues, suggesting that parkin overexpression effectively enhances mitochondrial function. This resonates with studies of a fly model of amyotrophic lateral sclerosis, where pan-neuronal expression of parkin was found to be protective by restoring complex I and complex III levels and assembly (Cha et al., 2020). In addition, in ageing mice, overexpressing parkin in muscles attenuated loss of muscle mass and strength by increasing mitochondrial enzymatic activities (Leduc-Gaudet et al., 2019) Indeed there is mounting evidence that parkin has a direct function in modulating metabolism, as seen, for example, in its ability to suppress the Warburg effect in tumorigenic cells, reducing glycolysis and promoting mitochondrial respiration (Zhang et al., 2011). Studies in mammalian cells suggest that parkin expression could be

favouring mitochondrial oxidative phosphorylation by upregulating the E1 α 1 subunit of the enzyme pyruvate dehydrogenase which links glycolysis to mitochondrial respiration (Zhang et al., 2011). When testing this hypothesis in flies however, we found that parkin expression, either in fly neurons or muscles, did not significantly alter levels of the pyruvate dehydrogenase E1 α 1 subunit.

Another scenario concerns the relationship between parkin, PARIS and the master regulator of mitochondrial biogenesis, PGC1- α . By downregulating the levels of PARIS, a repressor of PGC1- α , parkin expression would result in increased levels of PGC1- α , driving enhanced mitochondrial biogenesis and function (Pirooznia et al., 2020). However, in our study, immunoblotting the *Drosophila* PGC1- α homologue, spargel, failed to show deficiency of PGC1- α in HTT, and parkin overexpression had little effect on PGC1- α levels in HD and wild-type flies. Furthermore, an increase in PGC1- α would be expected to result in a corresponding increase in mitochondrial mass (Pirooznia et al., 2020). In fact, we observed the opposite, with HD flies presenting highly increased mitochondrial mass in the muscles, which was restored to normal control levels upon expression of parkin. Thus, the role of parkin in our fly HD model contrasts with observations made in *Drosophila* dopaminergic neurons, in which the protective role of parkin seems to be predominately due to its role in mitochondrial biogenesis via the PARIS/PGC1- α axis (Pirooznia et al., 2020).

We uncovered evidence that expressing parkin increased fission in the mitochondria of the flight muscle, compensating for the larger mitochondria that are packed between fibrils in the muscles of HD flies. In wild-type *Drosophila* pan-neuronal expression of parkin was previously shown to increase fission in the mitochondria of flight muscles (Rana et al., 2013). A second study, again in wild-type animals, observed that overexpression of Pink1/parkin in flight muscles promoted mitophagy and extended lifespan (Si et al., 2019). Overexpression of parkin has also been shown to increase fission and/or mitophagy in mice

skeletal muscle (Leduc-Gaudet et al., 2019) and in rat hippocampal neurons (Yu et al., 2011) thereby indicating its conserved role in regulating mitochondrial dynamics and function. Our observation of larger and more densely packed mitochondria in the muscles of HD flies seems to contradict previous findings in HD model systems in which mitochondria appeared more fragmented than in controls (Song et al., 2011; Costa et al., 2010; Guo et al., 2013). However, in line with our results, it has been observed that the muscles in a mini pig model of HD exhibit a higher density of mitochondria compared to controls (Rodinova et al., 2019). Moreover, accumulation of larger, fused mitochondria in fly indirect flight muscles is often a hallmark of ageing and disease (Deng et al., 2008; Rana et al., 2013; Rana et al., 2017; Scialo et al., 2016).

It is possible that in our HD model parkin expression ameliorates mitochondrial function simply by enhancing the selective removal of damaged mitochondria, which would help maintain a pool of healthy, functioning organelles. Consistent with this scenario, overexpression of parkin in heteroplasmic cybrid osteosarcoma cells was shown to selectively eliminate mitochondria that had deleterious mutations in cytochrome oxidase subunit I (COXI), sparing wild type mitochondria. The elimination of mitochondria with COXI mutations enriched the pool of wild type mitochondria, resulting in the rescue of cytochrome oxidase activity (Suen et al., 2010). Additionally Vincow et al. (2013) found that in *Drosophila*, the turnover of several mitochondrial respiratory chain subunits is impaired in parkin mutants and this is greater than in autophagy deficient *Atg7* mutants, indicating not only that parkin promotes mitophagy in vivo, but also that it is selective towards mitochondrial respiratory chain subunits in an autophagy-independent manner (Vincow et al., 2013). It is therefore of further interest that we observed that the expression of parkin in wild type flies per se did not increase mitochondrial respiration. Taken together with our lack of evidence that parkin modulates mitochondrial metabolism (see PDH and PGC1- α results discussed above), this suggests that parkin-mediated improvement of respiration in HTT flies is more likely to be due to the removal of dysfunctional organelles, resulting in the enhancement of the pool of healthy mitochondria.

A lack of mitophagy in mitochondria from the retina of HD model flies has been previously observed, and upregulation of Pink1 resulted in increased mitophagy and rescue of the neuronal associated HD phenotypes (Khalil et al., 2015). However, somewhat surprisingly, overexpression of parkin did not result in significant rescue of HD phenotypes (Khalil et al., 2015). In the same study the effects of increasing fission by upregulating Drp1 or inhibiting fusion by downregulating the fusion factor Marf proved ineffective in rescuing fly HD phenotypes. Here we also show that upregulating Pink1 is protective in several, but not all, of the HD phenotypes studied, and that increasing fission via Drp1 or inhibiting fusion by knockdown of Marf provide some rescue of neurodegeneration but no improvement in HD fly survival. Moreover, in our study we observed that upregulating Pink1 or altering mitochondrial dynamics by enhancing fission via Drp1 did not result in increased mitochondrial respiration in fly muscles.

Finally, we found that direct manipulation and enhancement of mitochondrial electron transport, which bypassed defective complexes, was highly protective. Using an alternative NADH dehydrogenase or an alternative oxidase to bypass either complex I or complex III-IV respectively, we demonstrated a direct involvement of these complexes in the rescue of fly HD related neurodegeneration phenotypes, and revealed that enhancement of the respiratory chain function proves highly protective in HD. Both Ndi1 and AOX have been expressed in *Drosophila* in order to circumvent oxidative phosphorylation defects (Cho et al., 2012; Vilain et al., 2012; Fernandez-Ayala et al., 2009; Kempainen et al., 2014; Humphrey et al., 2012; Vartiainen et al., 2014), and manipulate electron flow through the electron transport system (Scialo et al., 2016), proving protective in several disease models. However, in wild type *Drosophila* only expression of Ndi1 results in enhanced lifespan (Scialo et al., 2016; Bahadorani et al., 2010; Scialo et al., 2020; Sanz et al., 2010). Here we show that in HD flies enhancing

the flow of electrons to ubiquinone by Ndi1, or past the reduced ubiquinol with AOX, both result in a remarkable improvement of HTT93Q neuronal expression-related defects. We also show that Ndi1 or AOX expression have measurable effects on mitochondrial respiration both in HD and wild type fly neurons, significantly increasing the OXPHOS and ETS capacity through complex I or I and II.

As predicted from observations in previous studies (Juszczuk and Rychter, 2003; Hakkaart et al., 2006; Dassa et al., 2009b; Fernandez-Ayala et al., 2009; El-Khoury et al., 2013), we revealed that AOX-mediated bypassing of complex III-IV is accompanied by a notable reduction of mitochondrial ROS in the brain. ROS have long been implicated in ageing and neurodegeneration (Scialo et al., 2016; Sbdio et al., 2019; Scialo and Sanz, 2021), and while they also have important signalling functions and are implicated in extending the longevity of wild type flies (Scialo et al., 2016; Scialo et al., 2020), the protection conferred in HD flies by AOX or neuronal expression of Sod2, suggest that reducing mitochondrial ROS (mtROS) production could also be beneficial, although this warrants more detailed investigation.

Finally, we tested the effects of combining pan-neuronal expression of parkin with that of AOX in HTT flies. We found that simultaneous expression of park and AOX resulted in no significant improvement in any of the HD phenotypes tested when compared to the effects of expressing either parkin or AOX on their own. On the contrary, simultaneous expression of parkin and AOX in 7 day old HTT flies resulted in significantly fewer rhabdomeres when compared to HTT flies expressing only AOX. Furthermore, the median longevity of HTT flies expressing both parkin and AOX was significantly worse than that of HTT flies expressing only AOX. If parkin protection is due to the increase in the pool of healthy mitochondrial via fission/mitophagy, and AOX expression on its own results in healthier and better functioning mitochondria (as we see with increased OXPHOS and reduced ROS), combining expression of parkin and AOX might be detrimental due to increased fission by parkin in already AOX-mediated healthy mitochondria, thereby disturbing the delicate balance between fission and fusion.

In summary, our results underscore the therapeutic potential of targeting and bypassing mitochondrial dysfunction and the electron transport chain in HD, and open up a novel and promising avenue for ameliorating the severe phenotypes associated with this fatal disorder.

4. Materials and methods

4.1. *Drosophila* stocks

Fruit flies were raised and maintained on maize meal/glucose/yeast/agar medium (35:35:25:5%) to which nipagin and propionic acid were added, in a light-dark cycle (LD12:12) at 25 °C. The *elav-GAL4* [c155] (Stock # 458) and *Mef2-GAL4* drivers (Stock # 27390) were obtained from the Bloomington Stock Centre, Indiana. The *UASHTT93Q exon 1* (HTT93Q) lines P463 (insert on the third chromosome) and P468 (insert on the second chromosome - *HTT93Q(2)*) were gifts from Larry Marsh and Leslie Thompson (University of California, Irvine) (Steffan et al., 2001). The *Drosophila parkin* expressing line (Greene et al., 2003) was a gift from Miguel Martins (MRC Toxicology Unit, Leicester), and the second parkin line (*parkMyc*) was obtained from the Bloomington Stock Centre (Stock # 34748). The *UASPink1* line with the transgene on the second chromosome was a gift from Alex Whitworth (MRC Mitochondrial Biology Unit, Cambridge) and the *UASPink1* line with the transgene on the third chromosome (*Pink1(3)*) was obtained from the Bloomington Stock Centre (Stock # 51648). The *UASDrp1* line was obtained from the Bloomington Stock Centre (Stock # 51647) and the *Marf* RNAi line (VDRC ID # 105261) was obtained from the *phic31* KK RNAi Library, courtesy of the Vienna *Drosophila* RNAi Center. The AOX (Fernandez-Ayala et al., 2009) and *Ndi1* (Sanz et al., 2010) expressing lines were a gift from Howard T. Jacobs (Institute of Medical Technology and Tampere University Hospital, University of Tampere, Finland) and Alberto Sanz (Glasgow University, Institute of Molecular, Cell and

System Biology). The *UASSod2* line was obtained from the Bloomington Stock Centre (Stock # 24494).

4.2. Rhabdomere analysis

The number of visible rhabdomeres per ommatidium was scored using the pseudopupil assay (Campesan et al., 2011) for at least 50 ommatidia per fly, with 10–30 female flies examined per genotype at day 1 or 7 post-eclosion (the exact number of flies used per experiment is reported in the figure legends). Heads from aged flies were fixed to slides using fingernail polish, and rhabdomeres were examined at 50× magnification using either a Nikon Optiphot-2 or an Olympus BH2 microscope. As the maximum number of visible rhabdomeres per ommatidium is 7, percent rhabdomere rescue was calculated for each genotype as follows: $[(X-Y)/(7-Y)] \times 100$, where X = average rhabdomeres for an individual genotype, Y = average rhabdomeres for *elav > HTT93Q* flies.

4.3. Eclosion

The pan-neuronal driver *elavGAL4* we used is located on the X chromosome. We crossed female flies carrying the *UAS* transgene(s) of interest to male *elavGAL4* so that the female progeny would inherit both the sex-linked *elavGAL4* and the *UAS* transgenes (and therefore have pan-neuronal expression of the relevant gene under *UAS* control). The male progeny from this cross (which inherit their single X chromosome from their mother) would carry the non-driven *UAS* transgene(s) without *elavGAL4*. A minimum of 8 vials with such crosses were set up at 25 °C in each experiment. The number of female and male progeny eclosing within each vial was counted until the first generation had completely hatched and the mean ratio of females/males for each genotype was calculated.

4.4. Longevity

Newly hatched virgin females were placed in vials in groups of ten and moved to fresh food twice a week. The surviving number of flies were scored regularly until all flies had died. Survival curves were compared with log-rank (Mantel-Cox) test. A minimum of 60 to a maximum of 400 flies were analysed per genotype, the number used for each experiment is reported in the figure legends.

4.5. Transmission electron microscopy (TEM)

The thoraces of two-week old females were dissected in PBS at RT, fixed in 4% PFA, 2.5% glutaraldehyde, 0.1 M sodium cacodylate buffer (pH 7.4) and subsequently in 1% osmium tetroxide / 1.5% Potassium ferricyanide. Fixed thoraces were washed three times in de-ionised H₂O, followed by dehydration steps in ethanol (30%, 50%, 70%, 90% and 100%), and then infiltrated and embedded in modified Spurr's low viscosity resin, which was polymerized at 60 °C for 16 h. Ultra-thin (~70 nm) sections of the thoraces were cut using a Ultracut E Ultramicrotome (Reichert), collected onto copper mesh grids and stained first with 2% aqueous uranyl acetate for 30 mins, then lead citrate for 2 min. Sections of the indirect flight muscle were viewed on a JEOL JEM-1400 TEM at an acceleration voltage of 100 kV and images of 10,000× magnification were captured using a Megaview III digital camera with iTEM software.

Mitochondria were traced manually in Fiji (Schindelin et al., 2012) and the "Measure" function was used to calculate the area of each mitochondrion in various sections between muscle fibers. The total area of all the mitochondria contained in each section was calculated and divided by the area of the section (mito area/area section analysed). The number of mitochondria in each section was also divided by the area of the section (mito number/area section analysed). *N* = 3 thoraces per genotype, 25–49 sections and 203–743 mitochondria analysed per thorax (see legend in Fig. 2 for exact n).

4.6. Citrate synthase activity assay

Five two-week old female flies were homogenized for 60 s in 100 µl CellLytic MT Cell Lysis Reagent (Sigma Aldrich,UK) and debris was cleared from the lysate by centrifugation at 10,000 ×g for 10 mins at 4 °C. The lysate was diluted 5-fold in lysis reagent and used for both citrate synthase and BCA protein content assays.

Citrate synthase activity was assayed using the Citrate Synthase Assay Kit (Sigma Aldrich UK) on a 96 well plate according to manufacturer's instructions, with 6 biological repeats per genotype and each sample measured in triplicate. A FLUOstar plate reader (Omega, BMG Labtech UK) was used to monitor the change in absorption of 412 nm wavelength light after addition of oxaloacetate to each sample and the rate of change in absorbance during the linear phase of the reaction was used to calculate CS activity (µM / ml / min). CS activity of each sample was normalised to total protein content, quantified by BCA assay (Thermo Fisher).

4.7. Respirometry

High resolution respirometry was conducted using an Oroboros O2K (Oroboros Instruments, Austria). Usually, one female fly was homogenized in 80 µl respiration buffer (MiR05: 0.5 mM EGTA, 3 mM MgCl₂, 60 mM K-lactobionate, 20 mM taurine, 10 mM KH₂PO₄, 2.0 mM HEPES, 110 mM sucrose, and 1 g/l BSA, pH 7.1) per sample. Alternatively, in another set of experiments, an 80 µl sample from a homogenate of five females was used. Experiments using one 1-day old male, homogenized in 80 µl respiration buffer, were also conducted. Each sample was added to the Oroboros chamber containing 2 ml of MiR05. Mitochondrial LEAK (L), oxidative phosphorylation (OXPHOS) and electron transport system (ETS) capacities were measured using a modified substrate-uncoupler-inhibitor-titration (SUIT) protocol that consisted of multiple sequential injections at saturating concentrations (Pesta and Gnaiger, 2012).

Non-phosphorylating, complex I linked, LEAK (L) was measured after adding 5 mM pyruvate, 5 mM proline, and 1 mM malate to the samples. ADP-stimulated oxydative phosphorylating capacity (OXPHOS) linked to complex I (P CI) was then measured after injection of 1.25 mM ADP. To achieve maximal convergent electron flux through both complex I and II, 10 mM succinate and, in some of the experiments, 15 mM glycerol-3-phosphate, were added to each chamber (P CI + II, PCI + II + GP).

To assess electron transport system capacity, 0.5 µM carbonyl cyanide *m*-chlorophenyl hydrazone (CCCP) was titrated in 1 µl steps (ETS CI + II or ETS CI + II + GP). 0.5 µM rotenone was then added to inhibit complex I and measure ETS capacity through complex II (ETS CII). Residual oxygen consumption (non-mitochondrial respiration ROX) was then determined by adding 2.5 µM Antimycin A to inhibit complex III. For each experiment, the value of the leak (L) was subtracted from the oxphos (P) and ETS values and ROX measurements were subtracted from the value of the leak.

The electron transport system capacity of complex IV (ETS CIV) was measured after injection of 2 mM ascorbate +0.5 mM TMPD (*N,N,N,N*-tetramethyl-*p*-phenylenediamine dihydrochloride). Subsequent injection of 10 µM cytochrome *c* increased respiration and this increase was measured and termed "delta Cyt_c" (Δ Cyt_c). Auto-oxidation of TMPD was finally measured after addition of 100 mM sodium azide to block complex IV and this value was subtracted from the ETS CIV measurements.

4.8. Immunoblotting

When transgenes were expressed pan-neuronally via the *elav-GAL4* driver, protein lysates were obtained by homogenizing 35 one-week old fly heads in Ripa buffer (50 mM TrisHCl PH 7.4; 150 mM NaCl; 1% TritonX-100; 0.5% Sodium Deoxycholate; 0.1% SDS; 1 mM EDTA) + proteinase inhibitors (cComplete Protease Inhibitor Cocktail, Roche) and

centrifuging the homogenate at 16000 ×g for 20 min. Protein quantification was performed using the Bio-Rad DC Protein Assay. 20–50 µg of protein were separated on Novex™ WedgeWell™ 4 to 20%, Tris-Glycine Mini Protein Gels (Invitrogen UK) and wet-transferred to PVDF membrane. Membranes were blocked for 1 h in TBS-T + 5% milk and incubated at 4 °C overnight with primary antibodies (Antibodies used: 1:1000 mouse anti-Pyruvate Dehydrogenase E1-α subunit [8D10E6] ab110334; 1:5000 anti-Spargel Srl214AA–custom rabbit polyclonal antibody (George and Jacobs, 2019), a kind gift of H.T. Jacobs, Faculty of Medicine and Health Technology, Tampere University, Finland) and 1 h RT with 1:10000 horseradish peroxidase (HRP)-conjugated secondary antibody (Vector Laboratories). Membranes were washed 3 × 5 min in TBS-T after primary and secondary antibody incubations. HRP-conjugated secondary antibodies were detected using the Super Signal™ West Pico PLUS Chemiluminescent Substrate (Thermo Fisher UK) and imaged with the G:BOX imaging system (Syngene UK). Proteins were visualized using the No-Stain Protein Labeling Reagent (Invitrogen UK) allowing to perform total protein normalization.

When transgenes were expressed in fly muscles via the *Mef2-GAL4* driver, 5 two-week old female flies were homogenized in RIPA Buffer (Invitrogen UK) and protein concentrations were determined by BCA assay (Invitrogen UK). 10–20 µg of proteins per sample were separated on Novex 10% Tris-glycine gels (Invitrogen UK) or Novex™ Wedge-Well™ 4 to 20%, Tris-Glycine Mini Protein Gels (Invitrogen UK) and were transferred to PVDF membrane by wet transfer. Membranes were blocked for 1 h with 5% (w/v) milk protein in TBS-T (0.1% TWEEN20). Membranes were incubated with primary antibody (Antibodies used: 1:1000 mouse Anti-Pyruvate Dehydrogenase E1-α subunit antibody [8D10E6] ab110334, Abcam; and 1:10000 mouse anti-tubulin, Sigma) in 5% (w/v) milk at 4 °C overnight, and 1 h RT with 1:10000 horseradish peroxidase (HRP)-conjugated secondary antibody (Vector Laboratories). Membranes were washed 3 × 5 min in TBS-T (0.1% TWEEN20) after primary and secondary antibody incubations. HRP-conjugated secondary antibodies were detected using SuperSignal West PICO Plus Chemiluminescent substrate (Thermo Fisher UK) and imaged with the GeneGnome XRC imaging system (Syngene UK) or the G:BOX imaging system (Syngene UK).

4.9. ROS measurements with Mitosox

The brains of one-week old females were dissected in cold PBS and incubated in freshly prepared 5 µM Mitosox Red (Invitrogen UK) for 30 min at room temperature. The brains were then washed 3 times with PBS and mounted in Vectashield (Invitrogen UK), between a slide and a coverslip placed on double-sided tape to prevent squashing. Confocal laser scanner microscopy analysis (CLSM) analysis was performed using an Olympus FV1000 confocal laser scanning microscope. Brains were imaged using a 10× UPlanSAPO Olympus objective and Z-stacks were acquired through the entire thickness of the brain. Total fluorescent intensity was measured using Fiji. N: *elav > HTT93Q* = 35; *elav > HTT93Q + park* = 24; *elav > HTT93Q + AOX* = 18; *elavGAL4/+* = 24 brains.

4.10. Statistical analysis

Statistical analyses were performed using Prism 8 (GraphPad). Details of tests performed on individual experiments are described in the respective figure legends. When ANOVA was used, the data was tested for equality of variances (Brown-Forsythe and Bartlett's test) and for normality (Kolmogorov-Smirnov test) implemented in Prism. *Post-hoc* comparisons were performed using the Tukey, Newman-Keuls or Sidak's tests. Data with significant deviations from normality were analysed non-parametrically by Kruskal-Wallis ANOVA with Dunn's *post-hoc* comparisons.

CRedit authorship contribution statement

Susanna Campesan: Conceptualization, Investigation, Formal analysis, Writing – original draft, Writing – review & editing, Supervision, Funding acquisition. **Ivana del Popolo:** Investigation. **Kyriaki Marcou:** Investigation. **Anna Straatman-Iwanowska:** Investigation. **Mariaelena Repici:** Investigation. **Kalina V. Boytcheva:** Investigation. **Victoria E. Cotton:** Investigation. **Natalie Allcock:** Resources. **Ezio Rosato:** Resources. **Charalambos P. Kyriacou:** Writing – review & editing. **Flaviano Giorgini:** Conceptualization, Writing – review & editing, Supervision, Funding acquisition.

Declaration of Competing Interest

The authors have no conflicts of interest to declare.

Data availability

Data will be made available on request.

Acknowledgements

We acknowledge the Advanced Imaging Facility at the University of Leicester for support and thank Dr. Kees Straatman for helping with confocal imaging. We also thank the individuals and repositories that provided the various fly lines and antibodies utilized in this study. SC, MR, VEC and FG were supported by Medical Research Council research grants (MR/M013847/1; MR/L003503/1). KVB was supported by the Midlands Integrative Biosciences Training Partnership (MIBTP) funded by the Biotechnology and Biological Sciences Research Council.

Appendix A. Supplementary data

Supplementary data to this article can be found online at <https://doi.org/10.1016/j.nbd.2023.106236>.

References

- Andreassen, O.A., et al., 2001. Dichloroacetate exerts therapeutic effects in transgenic mouse models of Huntington's disease. *Ann. Neurol.* 50, 112–116. <https://doi.org/10.1002/ana.1085>.
- Antonini, A., et al., 1996. Striatal glucose metabolism and dopamine D2 receptor binding in asymptomatic gene carriers and patients with Huntington's disease. *Brain* 119 (Pt 6), 2085–2095. <https://doi.org/10.1093/brain/119.6.2085>.
- Aziz, N.A., et al., 2008. Weight loss in Huntington disease increases with higher CAG repeat number. *Neurology* 71, 1506–1513. <https://doi.org/10.1212/01.wnl.0000334276.09729.0e>.
- Bahadorani, S., et al., 2010. Neuronal expression of a single-subunit yeast NADH-ubiquinone oxidoreductase (Ndi1) extends *Drosophila* lifespan. *Aging Cell* 9, 191–202. <https://doi.org/10.1111/j.1474-9726.2010.00546.x>.
- Brouillet, E., et al., 1998. Partial inhibition of brain succinate dehydrogenase by 3-nitropropionic acid is sufficient to initiate striatal degeneration in rat. *J. Neurochem.* 70, 794–805. <https://doi.org/10.1046/j.1471-4159.1998.70020794.x>.
- Browne, S.E., 2008. Mitochondria and Huntington's disease pathogenesis: insight from genetic and chemical models. *Ann. N. Y. Acad. Sci.* 1147, 358–382. <https://doi.org/10.1196/annals.1427.018>.
- Browne, S.E., et al., 1997. Oxidative damage and metabolic dysfunction in Huntington's disease: selective vulnerability of the basal ganglia. *Ann. Neurol.* 41, 646–653. <https://doi.org/10.1002/ana.410410514>.
- Butterworth, J., Yates, C.M., Reynolds, G.P., 1985. Distribution of phosphate-activated glutaminase, succinic dehydrogenase, pyruvate dehydrogenase and gamma-glutamyl transpeptidase in post-mortem brain from Huntington's disease and agonal cases. *J. Neurol. Sci.* 67, 161–171. [https://doi.org/10.1016/0022-510x\(85\)90112-1](https://doi.org/10.1016/0022-510x(85)90112-1).
- Campesan, S., et al., 2011. The kynurenine pathway modulates neurodegeneration in a *Drosophila* model of Huntington's disease. *Curr. Biol.* 21, 961–966. <https://doi.org/10.1016/j.cub.2011.04.028>.
- Cha, S.J., et al., 2020. Parkin expression reverses mitochondrial dysfunction in fused in sarcoma-induced amyotrophic lateral sclerosis. *Insect Mol. Biol.* 29, 56–65. <https://doi.org/10.1111/imb.12608>.
- Chiang, M.-C., et al., 2010. Modulation of energy deficiency in Huntington's disease via activation of the peroxisome proliferator-activated receptor gamma. *Hum. Mol. Genet.* 19, 4043–4058. <https://doi.org/10.1093/hmg/ddq322>.

- Cho, J., Hur, J.H., Graniel, J., Benzer, S., Walker, D.W., 2012. Expression of yeast NDI1 rescues a *Drosophila* complex I assembly defect. *PLoS One* 7, e50644. <https://doi.org/10.1371/journal.pone.0050644>.
- Clark, I.E., et al., 2006. *Drosophila* pink1 is required for mitochondrial function and interacts genetically with parkin. *Nature* 441, 1162–1166. <https://doi.org/10.1038/nature04779>.
- Costa, V., et al., 2010. Mitochondrial fission and cristae disruption increase the response of cell models of Huntington's disease to apoptotic stimuli. *EMBO Mol. Med.* 2, 490–503. <https://doi.org/10.1002/emmm.201000102>.
- Cui, L., et al., 2006. Transcriptional repression of PGC-1 α by mutant huntingtin leads to mitochondrial dysfunction and neurodegeneration. *Cell* 127, 59–69. <https://doi.org/10.1016/j.cell.2006.09.015>.
- Dassa, E.P., Dufour, E., Goncalves, S., Jacobs, H.T., Rustin, P., 2009a. The alternative oxidase, a tool for compensating cytochrome c oxidase deficiency in human cells. *Physiol. Plant.* 137, 427–434. <https://doi.org/10.1111/j.1399-3054.2009.01248.x>.
- Dassa, E.P., et al., 2009b. Expression of the alternative oxidase complements cytochrome c oxidase deficiency in human cells. *EMBO Mol. Med.* 1, 30–36. <https://doi.org/10.1002/emmm.200900001>.
- De Vries, S., Van Witzenburg, R., Grivell, L.A., Marres, C.A.M., 1992. Primary structure and import pathway of the rotenone-insensitive NADH-ubiquinone oxidoreductase of mitochondria from *Saccharomyces cerevisiae*. *Eur. J. Biochem.* 203, 587–592. <https://doi.org/10.1111/j.1432-1033.1992.tb16587.x>.
- Deng, H., Dodson, M.W., Huang, H., Guo, M., 2008. The Parkinson's disease genes pink1 and parkin promote mitochondrial fission and/or inhibit fusion in *Drosophila*. *Proc. Natl. Acad. Sci. U. S. A.* 105, 14503–14508. <https://doi.org/10.1073/pnas.0803998105>.
- Djousse, L., et al., 2002. Weight loss in early stage of Huntington's disease. *Neurology* 59, 1325–1330. <https://doi.org/10.1212/01.wnl.00000031791.10922.cf>.
- Ehinger, J.K., Morota, S., Hansson, M.J., Paul, G., Elmer, E., 2016. Mitochondrial respiratory function in peripheral blood cells from huntington's disease patients. *Mov. Disord. Clin. Pract.* 3, 472–482. <https://doi.org/10.1002/mdc3.12308>.
- El-Khouri, R., et al., 2013. Alternative oxidase expression in the mouse enables bypassing cytochrome c oxidase blockade and limits mitochondrial ROS overproduction. *PLoS Genet.* 9, e1003182. <https://doi.org/10.1371/journal.pgen.1003182>.
- Feigin, A., et al., 2001. Metabolic network abnormalities in early Huntington's disease: an [(18)F]FDG PET study. *J. Nucl. Med.* 42, 1591–1595.
- Fernandez-Ayala, D.J., et al., 2009. Expression of the *Ciona* intestinalis alternative oxidase (AOX) in *Drosophila* complements defects in mitochondrial oxidative phosphorylation. *Cell Metab.* 9, 449–460. <https://doi.org/10.1016/j.cmet.2009.03.004>.
- Gegg, M.E., et al., 2010. Mitofusin 1 and mitofusin 2 are ubiquitinated in a PINK1/parkin-dependent manner upon induction of mitophagy. *Hum. Mol. Genet.* 19, 4861–4870. <https://doi.org/10.1093/hmg/ddq419>.
- George, J., Jacobs, H.T., 2019. Minimal effects of spargel (PGC-1) overexpression in a *Drosophila* mitochondrial disease model. *Biol. Open* 8. <https://doi.org/10.1242/bio.042135>.
- Glauser, L., Sonnay, S., Stafa, K., Moore, D.J., 2011. Parkin promotes the ubiquitination and degradation of the mitochondrial fusion factor mitofusin 1. *J. Neurochem.* 118, 636–645. <https://doi.org/10.1111/j.1471-4159.2011.07318.x>.
- Gnaiger, E., 2014. *Mitochondrial Pathways and Respiratory Control*, 4th edition edn. *Oroboros MiPNet Publications* 2014.
- Goebel, H.H., Heipertz, R., Scholz, W., Iqbal, K., Tellez-Nagel, I., 1978. Juvenile Huntington chorea: clinical, ultrastructural, and biochemical studies. *Neurology* 28, 23–31. <https://doi.org/10.1212/wnl.28.1.23>.
- Greene, J.C., et al., 2003. Mitochondrial pathology and apoptotic muscle degeneration in *Drosophila* parkin ** mutants. *Proc. Natl. Acad. Sci.* 100, 4078–4083. <https://doi.org/10.1073/pnas.0737556100>.
- Guo, X., et al., 2013. Inhibition of mitochondrial fragmentation diminishes Huntington's disease-associated neurodegeneration. *J. Clin. Invest.* 123, 5371–5388. <https://doi.org/10.1172/JCI70911>.
- Hakkaert, G.A., Dassa, E.P., Jacobs, H.T., Rustin, P., 2006. Allotopic expression of a mitochondrial alternative oxidase confers cyanide resistance to human cell respiration. *EMBO Rep.* 7, 341–345. <https://doi.org/10.1038/sj.embor.7400601>.
- Hargreaves, I.P., et al., 2007. Inhibition of mitochondrial complex IV leads to secondary loss complex II-III activity: implications for the pathogenesis and treatment of mitochondrial encephalomyopathies. *Mitochondrion* 7, 284–287. <https://doi.org/10.1016/j.mito.2007.02.001>.
- Humphrey, D.M., et al., 2012. Alternative oxidase rescues mitochondria-mediated dopaminergic cell loss in *Drosophila*. *Hum. Mol. Genet.* 21, 2698–2712. <https://doi.org/10.1093/hmg/dds096>.
- Jenkins, B.G., Koroshetz, W.J., Beal, M.F., Rosen, B.R., 1993. Evidence for impairment of energy metabolism in vivo in Huntington's disease using localized 1H NMR spectroscopy. *Neurology* 43, 2689. <https://doi.org/10.1212/wnl.43.12.2689>.
- Johri, A., Chandra, A., Flint Beal, M., 2013. PGC-1 α , mitochondrial dysfunction, and Huntington's disease. *Free Radic. Biol. Med.* 62, 37–46. <https://doi.org/10.1016/j.freeradbiomed.2013.04.016>.
- Juszczak, I.M., Rychter, A.M., 2003. Alternative oxidase in higher plants. *Acta Biochim. Pol.* 50, 1257–1271. doi:0350041257.
- Kemppainen, K.K., et al., 2014. Expression of alternative oxidase in *Drosophila* ameliorates diverse phenotypes due to cytochrome oxidase deficiency. *Hum. Mol. Genet.* 23, 2078–2093. <https://doi.org/10.1093/hmg/ddt601>.
- Khalil, B., et al., 2015. PINK1-induced mitophagy promotes neuroprotection in Huntington's disease. *Cell Death Dis.* 6, e1617. <https://doi.org/10.1038/cddis.2014.581>.
- Kosinski, C.M., et al., 2007. Myopathy as a first symptom of Huntington's disease in a Marathon runner. *Mov. Disord.* 22, 1637–1640. <https://doi.org/10.1002/mds.21550>.
- Larsen, S., et al., 2012. Biomarkers of mitochondrial content in skeletal muscle of healthy young human subjects. *J. Physiol.* 590, 3349–3360. <https://doi.org/10.1113/jphysiol.2012.230185>.
- Leduc-Gaudet, J.P., Reynaud, O., Hussain, S.N., Gouspillou, G., 2019. Parkin overexpression protects from ageing-related loss of muscle mass and strength. *J. Physiol.* 597, 1975–1991. <https://doi.org/10.1113/jp277157>.
- Lodi, R., et al., 2000. Abnormal in vivo skeletal muscle energy metabolism in Huntington's disease and dentatorubropallidolusian atrophy. *Ann. Neurol.* 48, 72–76.
- Mason, R.P., et al., 2013. Glutathione peroxidase activity is neuroprotective in models of Huntington's disease. *Nat. Genet.* 45, 1249–1254. <https://doi.org/10.1038/ng.2732>.
- Maxwell, D.P., Wang, Y., McIntosh, L., 1999. The alternative oxidase lowers mitochondrial reactive oxygen production in plant cells. *Proc. Natl. Acad. Sci. U. S. A.* 96, 8271–8276. <https://doi.org/10.1073/pnas.96.14.8271>.
- McColgan, P., Tabrizi, S.J., 2018. Huntington's disease: a clinical review. *Eur. J. Neurol.* 25, 24–34. <https://doi.org/10.1111/ene.13413>.
- McDonald, A.E., Vanlerberghe, G.C., 2004. Branched mitochondrial electron transport in the animalia: presence of alternative oxidase in several animal Phyla. *IUBMB Life* 56, 333–341. <https://doi.org/10.1080/1521-654040000876>.
- McDonald, A.E., Vanlerberghe, G.C., 2006. Origins, evolutionary history, and taxonomic distribution of alternative oxidase and plastoquinol terminal oxidase. *Comp. Biochem. Physiol. Part D Genom. Proteom.* 1, 357–364. <https://doi.org/10.1016/j.cbd.2006.08.001>.
- Mejia, E.M., Chau, S., Sparagna, G.C., Sipione, S., Hatch, G.M., 2016. Reduced mitochondrial function in human huntington disease lymphoblasts is not due to alterations in cardiolipin metabolism or mitochondrial supercomplex assembly. *Lipids* 51, 561–569. <https://doi.org/10.1007/s11745-015-4110-0>.
- Narendra, D., Tanaka, A., Suen, D.F., Youle, R.J., 2008. Parkin is recruited selectively to impaired mitochondria and promotes their autophagy. *J. Cell Biol.* 183, 795–803. <https://doi.org/10.1083/jcb.200809125>.
- Narendra, D.P., et al., 2010. PINK1 is selectively stabilized on impaired mitochondria to activate Parkin. *PLoS Biol.* 8, e1000298. <https://doi.org/10.1371/journal.pbio.1000298>.
- Orr, A.L., et al., 2008. N-terminal mutant huntingtin associates with mitochondria and impairs mitochondrial trafficking. *J. Neurosci.* 28, 2783–2792. <https://doi.org/10.1523/jneurosci.0106-08.2008>.
- Palfi, S., et al., 1996. Chronic 3-nitropropionic acid treatment in baboons replicates the cognitive and motor deficits of Huntington's disease. *J. Neurosci.* 16, 3019–3025.
- Pallos, J., et al., 2008. Inhibition of specific HDACs and sirtuins suppresses pathogenesis in a *Drosophila* model of Huntington's disease. *Hum. Mol. Genet.* 17, 3767–3775. <https://doi.org/10.1093/hmg/ddn273>.
- Park, J., et al., 2006. Mitochondrial dysfunction in *Drosophila* PINK1 mutants is complemented by parkin. *Nature* 441, 1157–1161. <https://doi.org/10.1038/nature04788>.
- Pesta, D., Gnaiger, E., 2012. High-resolution respirometry: OXPHOS protocols for human cells and permeabilized fibers from small biopsies of human muscle. *Methods Mol. Biol.* 810, 25–58. https://doi.org/10.1007/978-1-61779-382-0_3.
- Pirooznia, S.K., et al., 2020. PARIS induced defects in mitochondrial biogenesis drive dopamine neuron loss under conditions of parkin or PINK1 deficiency. *Mol. Neurodegener.* 15, 17. <https://doi.org/10.1186/s13024-020-00363-x>.
- Polyzos, A.A., McMurray, C.T., 2017. The chicken or the egg: mitochondrial dysfunction as a cause or consequence of toxicity in Huntington's disease. *Mech. Ageing Dev.* 161, 181–197. <https://doi.org/10.1016/j.mad.2016.09.003>.
- Poole, A.C., Thomas, R.E., Yu, S., Vincow, E.S., Pallanck, L., 2010. The mitochondrial fusion-promoting factor mitofusin is a substrate of the PINK1/parkin pathway. *PLoS One* 5, e10054. <https://doi.org/10.1371/journal.pone.0010054>.
- Puigserver, P., Spiegelman, B.M., 2003. Peroxisome proliferator-activated receptor- γ coactivator 1 α (PGC-1 α): transcriptional coactivator and metabolic regulator. *Endocr. Rev.* 24, 78–90. <https://doi.org/10.1210/er.2002-0012>.
- Rakovic, A., et al., 2011. Mutations in PINK1 and Parkin impair ubiquitination of Mitofusins in human fibroblasts. *PLoS One* 6, e16746. <https://doi.org/10.1371/journal.pone.0016746>.
- Rana, A., Rera, M., Walker, D., 2013. Parkin overexpression during aging reduces proteotoxicity, alters mitochondrial dynamics, and extends lifespan. *Proc. Natl. Acad. Sci. U. S. A.* 110. <https://doi.org/10.1073/pnas.1216197110>.
- Rana, A., et al., 2017. Promoting Drp1-mediated mitochondrial fission in midlife prolongs healthy lifespan of *Drosophila melanogaster*. *Nat. Commun.* 8, 448. <https://doi.org/10.1038/s41467-017-00525-4>.
- Reynolds Jr., N.C., Prost, R.W., Mark, L.P., 2005. Heterogeneity in 1H-MRS profiles of presymptomatic and early manifest Huntington's disease. *Brain Res.* 1031, 82–89. <https://doi.org/10.1016/j.brainres.2004.10.030>.
- Rodinova, M., et al., 2019. Deterioration of mitochondrial bioenergetics and ultrastructure impairment in skeletal muscle of a transgenic minipig model in the early stages of Huntington's disease. *Dis. Model. Mech.* 12. <https://doi.org/10.1242/dmm.038737>.
- Ross, C.A., Tabrizi, S.J., 2011. Huntington's disease: from molecular pathogenesis to clinical treatment. *Lancet Neurol.* 10, 83–98. [https://doi.org/10.1016/S1474-4422\(10\)70245-3](https://doi.org/10.1016/S1474-4422(10)70245-3).
- Saft, C., et al., 2005. Mitochondrial impairment in patients and asymptomatic mutation carriers of Huntington's disease. *Mov. Disord.* 20, 674–679. <https://doi.org/10.1002/mds.20373>.

- Sandoval, H., et al., 2014. Mitochondrial fusion but not fission regulates larval growth and synaptic development through steroid hormone production. *Elife* 3. <https://doi.org/10.7554/eLife.03558>.
- Sanz, A., et al., 2010. Expression of the yeast NADH dehydrogenase Ndi1 in *Drosophila* confers increased lifespan independently of dietary restriction. *Proc. Natl. Acad. Sci. U. S. A.* 107, 9105–9110. <https://doi.org/10.1073/pnas.0911539107>.
- Sbodio, J.L., Snyder, S.H., Paul, B.D., 2019. Redox mechanisms in neurodegeneration: from disease outcomes to therapeutic opportunities. *Antioxid. Redox Signal.* 30, 1450–1499. <https://doi.org/10.1089/ars.2017.7321>.
- Schindelin, J., et al., 2012. Fiji: an open-source platform for biological-image analysis. *Nat. Methods* 9, 676–682. <https://doi.org/10.1038/nmeth.2019>.
- Scialo, F., Sanz, A., 2021. Coenzyme Q redox signalling and longevity. *Free Radic. Biol. Med.* 164, 187–205. <https://doi.org/10.1016/j.freeradbiomed.2021.01.018>.
- Scialo, F., et al., 2016. Mitochondrial ROS produced via reverse Electron transport extend animal lifespan. *Cell Metab.* 23, 725–734. <https://doi.org/10.1016/j.cmet.2016.03.009>.
- Scialò, F., et al., 2020. Mitochondrial complex I derived ROS regulate stress adaptation in *Drosophila melanogaster*. *Redox Biol.* 32, 101450 <https://doi.org/10.1016/j.redox.2020.101450>.
- Seo, B.B., Wang, J., Flotte, T.R., Yagi, T., Matsuno-Yagi, A., 2000. Use of the NADH-quinone oxidoreductase (NDI1) gene of *Saccharomyces cerevisiae* as a possible cure for complex I defects in human cells. *J. Biol. Chem.* 275, 37774–37778. <https://doi.org/10.1074/jbc.M007033200>.
- Seo, B.B., Nakamaru-Ogiso, E., Flotte, T.R., Matsuno-Yagi, A., Yagi, T., 2006. In vivo complementation of complex I by the yeast Ndi1 enzyme. Possible application for treatment of Parkinson disease. *J. Biol. Chem.* 281, 14250–14255. <https://doi.org/10.1074/jbc.M600922200>.
- Shimura, H., et al., 2000. Familial Parkinson disease gene product, parkin, is a ubiquitin-protein ligase. *Nat. Genet.* 25, 302–305. <https://doi.org/10.1038/77060>.
- Shin, J.H., et al., 2011. PARIS (ZNF746) repression of PGC-1 α contributes to neurodegeneration in Parkinson's disease. *Cell* 144, 689–702. <https://doi.org/10.1016/j.cell.2011.02.010>.
- Si, H., et al., 2019. Overexpression of pink1 or parkin in indirect flight muscles promotes mitochondrial proteostasis and extends lifespan in *Drosophila melanogaster*. *PLoS One* 14, e0225214. <https://doi.org/10.1371/journal.pone.0225214>.
- Small, W.C., McAlister-Henn, L., 1998. Identification of a cytosolically directed NADH dehydrogenase in mitochondria of *Saccharomyces cerevisiae*. *J. Bacteriol.* 180, 4051–4055.
- Song, W., et al., 2011. Mutant huntingtin binds the mitochondrial fission GTPase dynamin-related protein-1 and increases its enzymatic activity. *Nat. Med.* 17, 377–382. <https://doi.org/10.1038/nm.2313>.
- Sorbi, S., Bird, E.D., Blass, J.P., 1983. Decreased pyruvate dehydrogenase complex activity in Huntington and Alzheimer brain. *Ann. Neurol.* 13, 72–78. <https://doi.org/10.1002/ana.410130116>.
- Squitieri, F., et al., 2006. Severe ultrastructural mitochondrial changes in lymphoblasts homozygous for Huntington disease mutation. *Mech. Ageing Dev.* 127, 217–220. <https://doi.org/10.1016/j.mad.2005.09.010>.
- Squitieri, F., et al., 2010. Abnormal morphology of peripheral cell tissues from patients with Huntington disease. *J. Neural Transm. (Vienna)* 117, 77–83. <https://doi.org/10.1007/s00702-009-0328-4>.
- Steffan, J.S., et al., 2001. Histone deacetylase inhibitors arrest polyglutamine-dependent neurodegeneration in *Drosophila*. *Nature* 413, 739–743. <https://doi.org/10.1038/35099568>.
- Steinert, J.R., et al., 2012. Rab11 rescues synaptic dysfunction and behavioural deficits in a *Drosophila* model of Huntington's disease. *Hum. Mol. Genet.* 21, 2912–2922. <https://doi.org/10.1093/hmg/dd117>.
- Suen, D.-F., Narendra, D.P., Tanaka, A., Manfredi, G., Youle, R.J., 2010. Parkin overexpression selects against a deleterious mtDNA mutation in heteroplasmic cybrid cells. *Proc. Natl. Acad. Sci.* 107, 11835–11840. <https://doi.org/10.1073/pnas.0914569107>.
- Tanaka, A., et al., 2010. Proteasome and p97 mediate mitophagy and degradation of mitofusins induced by Parkin. *J. Cell Biol.* 191, 1367–1380. <https://doi.org/10.1083/jcb.201007013>.
- Tellez-Nagel, I., Johnson, A.B., Terry, R.D., 1974. Studies on brain biopsies of patients with Huntington's chorea. *J. Neuropathol. Exp. Neurol.* 33, 308–332. <https://doi.org/10.1097/00005072-197404000-00008>.
- Trushina, E., et al., 2004. Mutant huntingtin impairs axonal trafficking in mammalian neurons in vivo and in vitro. *Mol. Cell. Biol.* 24, 8195–8209. <https://doi.org/10.1128/mcb.24.18.8195-8209.2004>.
- Tsunemi, T., La Spada, A.R., 2012. PGC-1 α at the intersection of bioenergetics regulation and neuron function: from Huntington's disease to Parkinson's disease and beyond. *Prog. Neurobiol.* 97, 142–151. <https://doi.org/10.1016/j.pneurobio.2011.10.004>.
- Vartiainen, S., et al., 2014. Phenotypic rescue of a *Drosophila* model of mitochondrial ANT1 disease. *Dis. Model. Mech.* 7, 635–648. <https://doi.org/10.1242/dmm.016527>.
- Vilain, S., et al., 2012. The yeast complex I equivalent NADH dehydrogenase rescues pink1 mutants. *PLoS Genet.* 8, e1002456 <https://doi.org/10.1371/journal.pgen.1002456>.
- Vincow, E.S., et al., 2013. The PINK1–Parkin pathway promotes both mitophagy and selective respiratory chain turnover in vivo. *Proc. Natl. Acad. Sci.* 110, 6400–6405. <https://doi.org/10.1073/pnas.1221132110>.
- Vives-Bauza, C., et al., 2010. PINK1-dependent recruitment of Parkin to mitochondria in mitophagy. *Proc. Natl. Acad. Sci.* 107, 378–383. <https://doi.org/10.1073/pnas.0911187107>.
- Watts, J.A., Kline, J.A., Thornton, L.R., Grattan, R.M., Brar, S.S., 2004. Metabolic dysfunction and depletion of mitochondria in hearts of septic rats. *J. Mol. Cell. Cardiol.* 36, 141–150. <https://doi.org/10.1016/j.yjmcc.2003.10.015>.
- Weydt, P., et al., 2006. Thermoregulatory and metabolic defects in Huntington's disease transgenic mice implicate PGC-1 α in Huntington's disease neurodegeneration. *Cell Metab.* 4, 349–362. <https://doi.org/10.1016/j.cmet.2006.10.004>.
- Yang, Y., et al., 2006. Mitochondrial pathology and muscle and dopaminergic neuron degeneration caused by inactivation of *Drosophila* Pink1 is rescued by Parkin. *Proc. Natl. Acad. Sci. U. S. A.* 103, 10793–10798. <https://doi.org/10.1073/pnas.0602493103>.
- Yano, H., et al., 2014. Inhibition of mitochondrial protein import by mutant huntingtin. *Nat. Neurosci.* 17, 822–831. <https://doi.org/10.1038/nn.3721>.
- Youle, R.J., Narendra, D.P., 2011. Mechanisms of mitophagy. *Nat. Rev. Mol. Cell Biol.* 12, 9–14. <https://doi.org/10.1038/nrm3028>.
- Yu, W., Sun, Y., Guo, S., Lu, B., 2011. The PINK1/Parkin pathway regulates mitochondrial dynamics and function in mammalian hippocampal and dopaminergic neurons. *Hum. Mol. Genet.* 20, 3227–3240. <https://doi.org/10.1093/hmg/ddr235>.
- Zhang, C., et al., 2011. Parkin, a p53 target gene, mediates the role of p53 in glucose metabolism and the Warburg effect. *Proc. Natl. Acad. Sci. U. S. A.* 108, 16259–16264. <https://doi.org/10.1073/pnas.1113884108>.
- Zielonka, D., Piotrowska, I., Marcinkowski, J.T., Mielcarek, M., 2014. Skeletal muscle pathology in Huntington's disease. *Front. Physiol.* 5 <https://doi.org/10.3389/fphys.2014.00380>.
- Ziviani, E., Tao, R.N., Whitworth, A.J., 2010. *Drosophila* Parkin requires PINK1 for mitochondrial translocation and ubiquitinates Mitofusin. *Proc. Natl. Acad. Sci.* 107, 5018–5023. <https://doi.org/10.1073/pnas.0913485107>.